Transition zone assembly and its contribution to axoneme formation in *Drosophila* male germ cells

Jennifer Vieillard, Marie Paschaki, Jean-Luc Duteyrat, Céline Augière, Elisabeth Cortier, Jean-André Lapart, Joëlle Thomas,* and Bénédicte Durand*

Université Claude Bernard Lyon 1, Institut National de la Santé et de la Recherche Médicale U1217, Institut NeuroMyoGène, Centre National de la Recherche Scientifique UMR 5310, F-69100 Lyon, France

The ciliary transition zone (TZ) is a complex structure found at the cilia base. Defects in TZ assembly are associated with human ciliopathies. In most eukaryotes, three protein complexes (CEP290, NPHP, and MKS) cooperate to build the TZ. We show that in *Drosophila melanogaster*, mild TZ defects are observed in the absence of MKS components. In contrast, Cby and Azi1 cooperate to build the TZ by acting upstream of Cep290 and MKS components. Without Cby and Azi1, centrioles fail to form the TZ, precluding sensory cilia assembly, and no ciliary membrane cap associated with sperm ciliogenesis is made. This ciliary cap is critical to recruit the tubulin-depolymerizing kinesin Klp59D, required for regulation of axonemal growth. Our results show that *Drosophila* TZ assembly in sensory neurons and male germ cells involves cooperative actions of Cby and Dila. They further reveal that temporal control of membrane cap assembly by TZ components and microtubule elongation by kinesin-13 is required for axoneme formation in male germ cells.

Introduction

Cilia and flagella are highly conserved organelles involved in various cellular and physiological processes. Defects in cilia assembly are responsible for many human diseases (Badano et al., 2006; Baker and Beales, 2009; Brown and Witman, 2014). Cilia are built around a microtubule core, the axoneme, which grows from the basal body (BB), itself derived from the mother centriole. At the interface between the BB and the plasma membrane, a particular compartment, the transition zone (TZ), plays both structural and functional roles by regulating the traffic in and out of the cilium and by forming structural links between microtubules and the membrane (Hu and Nelson, 2011; Szymanska and Johnson, 2012). Several ciliopathies, such as the Joubert syndrome and the Meckel syndrome (MKS) or nephronophthisis (NPHP) are caused by defects in TZ components (Czarnecki and Shah, 2012).

TZ assembly is a complex process starting with the docking of the mother centriole to cytoplasmic vesicles and the timely and spatially ordered assembly of multiple proteins. TZ components have been extensively described in several organisms (Szymanska and Johnson, 2012). Genetic approaches in *Caenorhabditis elegans* (Williams et al., 2011) and biochemical approaches in mammalian cells helped to establish a first comprehensive hierarchy of these components (Chih et al., 2011; Garcia-Gonzalo et al., 2011; Sang et al., 2011). They fall into different modules, namely MKS, NPHP, and CEP290. Proteins of the MKS module colocalize and together contribute to the formation of the TZ in various organisms, from *C. elegans* to mammals. In *C. elegans*, MKS, NPHP, and CEP290 cooperate to assemble the TZ (Williams et al., 2011; Jensen et al., 2015; Schouteden et al., 2015; Yee et al., 2015). Upstream, MKS5 (mammalian Rpgrip1L or NPHP8) controls the assembly of the MKS and NPHP complexes on centrioles (Jensen et al., 2015; Schouteden et al., 2015; Li et al., 2016). However, variations exist between model organisms, and all TZ components are not conserved in all ciliated species. For example, MKS5 and several other NPHP proteins are absent from the *Drosophila melanogaster* genome (Barker et al., 2014). Additional components of the TZ have been identified, but their integration in the hierarchy of TZ assembly is not yet clear. For instance, Chibby (Cby) is a component of the TZ in *Drosophila* and vertebrates (Voronina et al., 2009; Enjolras et al., 2012; Lee et al., 2014; Shi et al., 2014), but how Cby contributes to TZ assembly remains to be characterized. Cby is absent from *C. elegans* and protozoa genomes (Enjolras et al., 2012). Dila (Azi1 in mammals) is also not present in *C. elegans* but is required for TZ assembly in *Drosophila* or for ciliogenesis in mammals and is also associated with centriolar satellites in vertebrates (Ma and Jarman, 2011; Hall et al., 2013; Villumsen et al., 2013; Chamling et al., 2014). Therefore, key components of TZ assembly in *C. elegans* or mammals such as MKS5 are missing in

*J. Thomas and B. Durand contributed equally to this paper.

Correspondence to Bénédicte Durand: durand-b@univ-lyon1.fr

Abbreviations used: 3D-SIM, 3D structured-illumination microscopy; BB, basal body; CBY, Chibby; DILA, Dilatory; IF, immunofluorescence; IFT, intraflagellar transport; KD, knockdown; MKS, Meckel syndrome; NPHP, nephronophthisis; TZ, transition zone; UNC, Uncoordinated.

The Rockefeller University Press $30.00
J. Cell Biol. Vol. 214 No. 7 875–889
www.jcb.org/cgi/doi/10.1083/jcb.201603086

Drosophila, and the mechanisms of TZ assembly in this organism are largely unknown.

Two main ciliated tissues are found in *Drosophila*: sensory neurons, in which cilia are required for transducing most senses, and sperm germ cells (Gogendeau and Basto, 2010). Sensory cilia assembly relies on intraflagellar transport (IFT) and is hence compartmentalized in *Drosophila* (Han et al., 2003; Sarpal et al., 2003). In contrast, flagella assembly in male germ cells is IFT independent and said to be cytosolic (Han et al., 2003; Sarpal et al., 2003; Basiri et al., 2014; Avidor-Reiss and Leroux, 2015). Such cytosolic mode of assembly is also proposed in mammals for the formation of the sperm midpiece (Avidor-Reiss and Leroux, 2015). In *Drosophila*, cytosolic flagella extension takes place inside a membrane ciliary cap, which requires Cep290 for proper organization and architecture (Basiri et al., 2014). This membrane cap is built in G2 *Drosophila* spermatocytes, when all four replicated centrioles dock to the plasma membrane and grow a primary cilium. During meiosis, the four primary cilia are internalized together with centrioles, maintaining the membrane ciliary cap connected to the plasma membrane (Tates, 1971; Carvalho-Santos et al., 2012; Riparbelli et al., 2012; Jana et al., 2016).

Here, we show that MKS proteins are involved in *Drosophila* TZ assembly, but simultaneous removal of several MKS components only leads to very mild TZ and axonemal defects. Instead, deleting both Cby and Dila, two components of the TZ in *Drosophila*, leads to extremely severe TZ disorganization with complete loss of MKS components and severe reduction of Cep290. In absence of Cby and Dila, BBs fail to dock to the plasma membrane of spermatocytes and assemble the ciliary membrane cap required for sperm flagella elongation. In absence of this ciliary cap, aberrant growth of axonemal microtubules is observed in spermatocytes. We demonstrate that Klp59D, a kinesin-13 family member, is present at the ciliary cap and is required for proper and timely regulated growth of the axoneme. We therefore propose that the ciliary cap is necessary to restrict and timely coordinate ciliary component assembly in *Drosophila* spermatocytes.

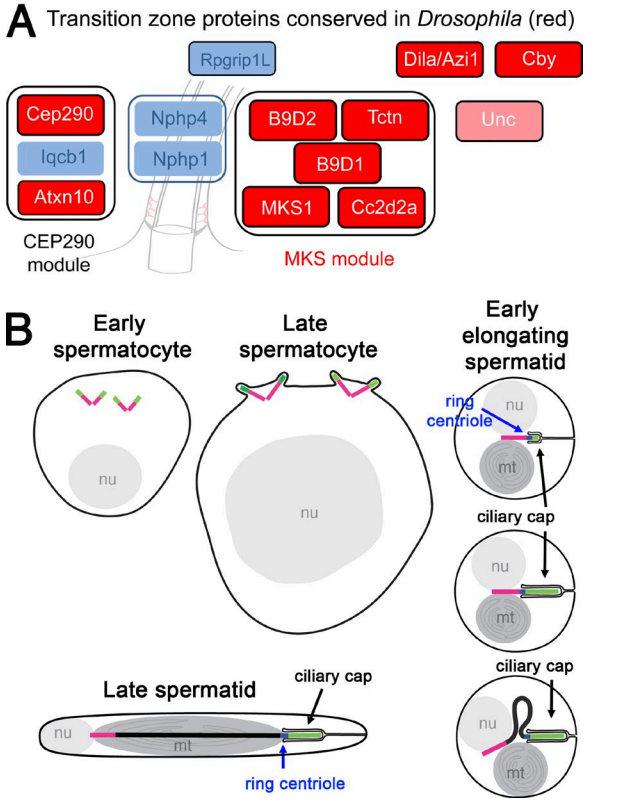

Figure 1. **TZ components in *Drosophila* and scheme of spermatogenesis.** (A) Scheme of TZ components present in mammals assigned in different functional modules. Conserved proteins in *Drosophila* are in red, not conserved in blue. Unc is present in *Drosophila*, not in mammals. (B) Scheme representing centrioles/basal bodies (BBs) at different stages of male germ cells. In early spermatocytes, the two pairs of centrioles (magenta) start to accumulate TZ components (green) at their tips. During spermatocyte maturation, centrioles convert to BBs (magenta), dock to the plasma membrane, and extend cilia/TZ (green). During meiosis, BBs and cilia/TZ are internalized, keeping the ciliary cap connected to the plasma membrane. In round spermatids, the BBs are apposed to the nuclei and extend the ciliary cap (green) connected to the plasma membrane. Ring centriole (blue) connects the base of the ciliary cap to the centriole. Starting axoneme elongation, the ciliary cap is extended, the axoneme grows (black), and the ciliary cap and ring centriole progressively migrate away from the BB.

Results

Organization of TZ components in *Drosophila*

In mammals and *C. elegans*, three protein complexes (MKS, NPHP, and CEP290) have been shown to be key players of TZ assembly. CEP290 and most MKS module proteins are conserved in *Drosophila,* whereas most NPHP components are missing (Fig. 1 A). In addition, Cby and Dila, two proteins conserved in mammals, were shown to be located at the TZ and involved in cilia assembly in *Drosophila* (Ma and Jarman, 2011; Enjolras et al., 2012). To understand more precisely how these components work together, we tagged several MKS proteins and compared their distribution in relation to Cby and Dila. We previously showed that B9d1 colocalizes with Cby in embryonic sensory cilia (Enjolras et al., 2012). Here, we show that the other members of the MKS module, B9d2, Mks1/B9d3, Tectonic (Tctn), and Cc2d2a, are found at the TZ at the base of sensory cilia as illustrated in chordotonal neurons of the antennae (Fig. S1).

In male germ cells, a dynamic behavior of centrioles and cilia takes place (Fig. 1 B). In midstage spermatocytes, all four centrioles dock to the plasma membrane and primary cilia like structures are extended at the surface of late spermatocytes (Tates, 1971; Carvalho-Santos et al., 2012; Riparbelli et al., 2012). Using superresolution 3D structured-illumination microscopy (3D-SIM), we observed that from early to late spermatocytes, Cby completely overlaps with acetylated tubulin (Fig. 2 A). Moreover, Mks1 (Fig. 2 D) colocalizes with Cby at the TZ. Membrane staining also reveals that Cby extends into the entire membrane cap in spermatocytes (Fig. 2 E). These results show that TZ and primary cilia are mingled at this stage, indicating that the primary cilium has a TZ composition.

The centrioles and cilia are next engulfed during meiosis (Tates, 1971; Fabian and Brill, 2012). In round spermatids, the centriole/BB still extends into the internalized ciliary membrane cap that is linked to the plasma membrane (Fig. 1 B). At the onset of flagellar axoneme elongation, the ciliary cap elongates and migrates opposite to the nucleus as a result of flagellum extension (Tates, 1971; Basiri et al., 2014). A particular structure called the ring centriole has been described in spermatids of many insects and corresponds to the base of the ciliary cap in elongating spermatids (Phillips, 1970; Fig. 1 B).

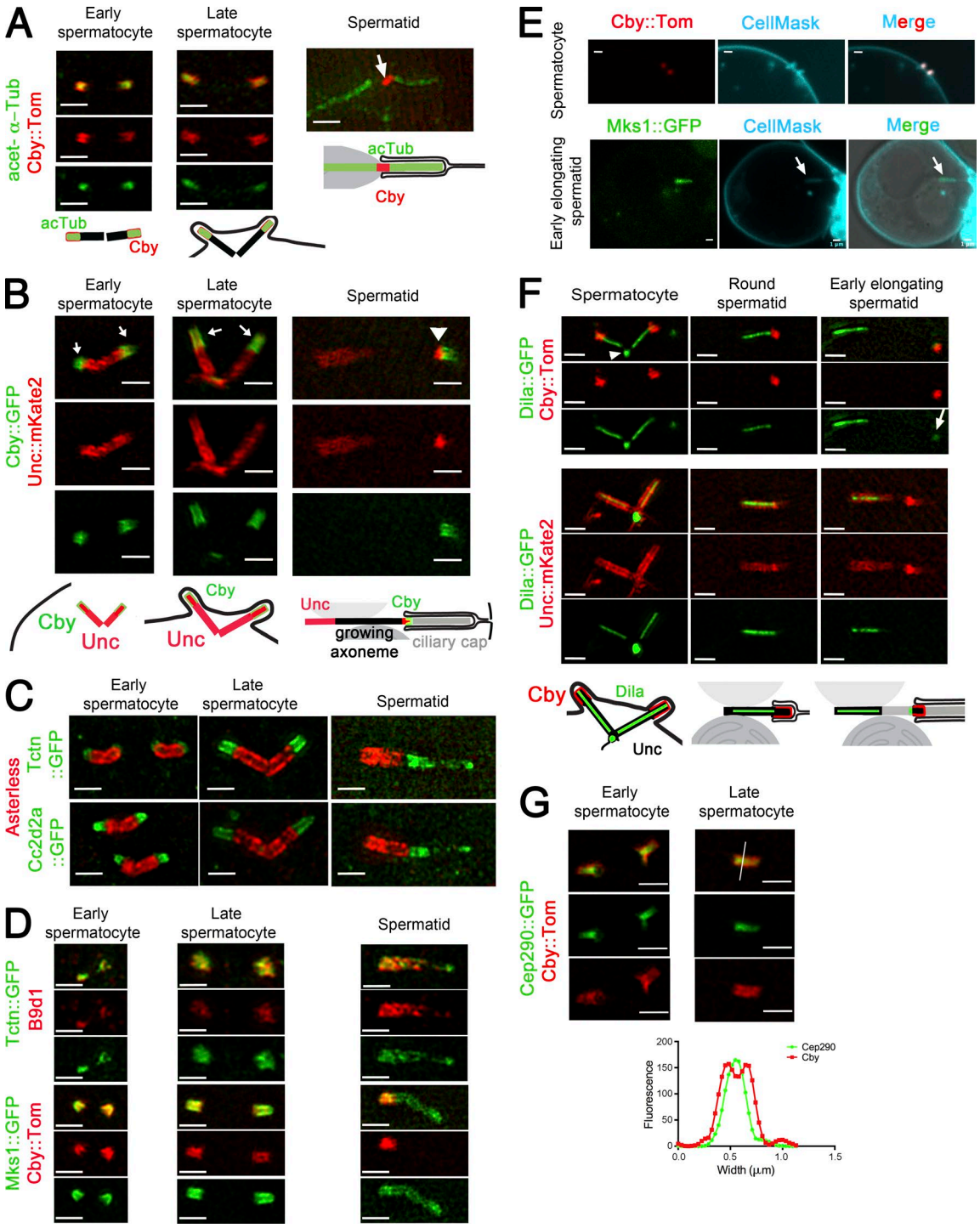

Figure 2. **Localization of TZ components in *Drosophila* male germ cells.** (A–D, F, and G) 3D-SIM imaging of male germ cells. Recapitulating schemes are based on Fig. 1. (A) Acetylated tubulin (acTub) and Cby overlap in spermatocytes. In elongating spermatids, Cby is restricted to the ring centriole (arrow), and acetylated tubulin stains the axoneme proximal and distal to the ring centriole. (B) Unc labels the BB, and Cby and Unc colocalize along the TZ/cilia (arrows). The ring centriole labeled with Unc and Cby (arrowhead) separates from the BB in elongating spermatids. (C and D) Tctn, Cc2d2a, B9d1, and Mks1 colocalize at the tip of the centrioles (Asl, red) and overlap with Cby in spermatocytes. In early elongating spermatids, all MKS components cover the entire ciliary cap, whereas Cby is restricted to the ring centriole. (E) Live confocal imaging of Cby and Mks1. Membranes are labeled with CellMask. Cby labels entirely the cilia/TZ in spermatocytes, and Mks1 labels the entire ciliary cap (arrows) in spermatids. (F) Dila covers the entire lumen of centriole and projects into the TZ/cilia marked by Cby or Unc in spermatocytes and round spermatids. Dila is at the base of centrioles (arrowhead), and a small fraction migrates with the ring centriole in the spermatid (arrow; gamma was adjusted to 1.35 for the green layer). (G) Cby surrounds Cep290 both at the TZ/cilia and at the ring centriole as observed on a scan profile of fluorescence intensity (grayscale units) across (white line) the TZ/ring centriole. Bars, 1 µm.

Previous observations showed that the ring centriole is marked by Unc and Cby (Baker et al., 2004; Enjolras et al., 2012; Gottardo et al., 2013) and this is confirmed here by comparing Cby to acetylated tubulin staining (Fig. 2 A, spermatid).

To understand more in details the organization of the TZ in spermatocytes and spermatids, we used superresolution 3D-SIM. In spermatocytes, we observed that Unc marks the whole centriole and cilium/TZ. Moreover, Cby and Unc radially overlap in the cilium/TZ (Fig. 2 B, arrows), but Cby extends a little more distally to Unc. MKS components Cc2d2a, Tctn, B9d1, and Mks1 (Fig. 2, C and D) are restricted to the cilium/TZ, distal to the centriole (Asterless [Asl]), where they overlap with Cby. Dila distribution was found to be very different from other TZ components. It is localized inside the centriole and also inside the cilium/TZ lumen and capped by Cby (Fig. 2 F). Dila also strongly stains an unknown round shaped structure (Fig. 2 F, arrowhead) at the base of some centriole pairs. Last, Cby is found more radially to Cep290 (Fig. 2 G).

In spermatids, a dynamic remodeling of TZ components is observed at the onset of flagella elongation: whereas Cby and a ring of Unc separate from the BB (Fig. 2 B, arrowhead) MKS components are redistributed all along the membrane cap that is extended at this stage, as observed both on high-resolution images (Fig. 2, C and D) and by live imaging (Fig. 2 E and Fig. S2). Note that costaining of MKS proteins with Cby showed that these components are enriched at ring centriole but also extend distal to Unc and Cby all along the ciliary cap. Dila is maintained, like Unc, at the BB, and a very small fraction of Dila is sometimes detected at the ring centriole, apposed to Cby (Fig. 2 F). Dila is disassembled from both the BB and the TZ soon after initiation of spermatid elongation. All other ciliary cap and ring centriole components (Cby, Mks1, B9d1-2, Tctn, Cd2d2A, and Unc) are disassembled from flagellar tips at the onset of sperm individualization.

Absence of *Drosophila* MKS module at the TZ only mildly affects cilia assembly

To understand the function of the MKS module, we created by CRISPR-Cas9–mediated homologous recombination a null allele of simultaneously *B9d2* and *tectonic* (*tctn*), as these two genes overlap in the genome (Fig. 3 A). *B9d2, tctn*$^{\Delta}$ flies are viable and do not show sensory behavioral defects. Males produce motile sperm and show only slightly reduced fertility (mean progeny per male: 99 [control] and 84 [*B9d2, tctn*$^{\Delta}$]; Fig. 3 B). In agreement with these observations, ultrastructural analysis of the antennae chordotonal cilia did not reveal structural defects of the axoneme or of the TZ (Fig. 3 C). We still observe transition fibers and Y-like linkers connecting, respectively, the centriole or axoneme to the plasma membrane in both control and *B9d2, tctn*$^{\Delta}$ flies. However, because these structures are difficult to observe in *Drosophila*, we cannot totally exclude that subtle ultrastructural defects could occur in absence of the MKS complex. In contrast, sperm flagella show weakly penetrant but statistically significant ultrastructural defects (Fig. 3 D). Approximately 10% of sperm flagella are broken or disorganized (Fig. 3 E), showing that Tctn and B9d2 are somehow involved in building stable axonemes.

We next analyzed the molecular organization of the TZ in absence of B9d2 and Tctn (Figs. 4 and S1). Cby and Cep290 are still recruited at the TZ (Fig. 4, A and B). We measured both the length of the centriole, labeled for Asl, and the length of the TZ labeled with Cep290 or Cby in absence of B9d2 and Tctn (Fig. 4 C), and we observed a small but significant decrease of TZ length that was correlated with an increase in centriole size. Strikingly, we observed a complete disruption of the MKS complex, as Mks1 and B9d1 are not recruited to the TZ in *B9d2, tctn*$^{\Delta}$ spermatocytes (Fig. 4, D and E). B9d1 localization was rescued by reintroducing both *tctn* and *B9d2* (Fig. 4 F). This shows that B9d2 and Tctn proteins are required to organize the MKS complex and that the absence of several proteins of the MKS complex at the TZ is largely dispensable for cilia assembly (Fig. 4 G). Based on this observation, we conclude that the MKS complex alone has only a subtle role in the organization of the TZ and ciliary cap in *Drosophila* sperm cells.

Cby and Dila cooperate to build the *Drosophila* TZ

In contrast to the weak impact of MKS protein deficiency on TZ assembly, mutations in proteins localized at the ring centriole lead to more severe phenotypes. Mutations in *unc*, *cby*, *dila*, or c*ep290* provoke marked uncoordination phenotypes caused by defects in ciliated neurons of the peripheral nervous system and show severe male infertility (Baker et al., 2004; Ma and Jarman, 2011; Enjolras et al., 2012; Basiri et al., 2014). Defects in Unc, Cby, and Dila lead to marked disorganization of sensory cilia, but BB still dock and build a TZ with only mild (Unc and Cby, showing interrupted distal segment of the TZ) or even no ultrastructural defects (Dila). The ultrastructure of sensory cilia was not investigated in *cep290* mutants. In spermatids, loss of Cep290 modifies the MKS protein distribution at the ciliary cap (Basiri et al., 2014).

Strikingly, when we combined *cby* and *dila* mutations, we observed severe consequences on the function and architecture of sensory neurons. Flies are completely uncoordinated and cilia are absent in chordotonal neurons as observed by immunofluorescence (IF) and EM analyzes (Fig. 5, A and B). Centrioles fail to build a TZ (Fig. 5, B and C), and Cep290 and Mks1 are absent at dendritic tips (Fig. 5 E). In *dila*^{81}*; cby*^{1} double mutants, we did not manage to observe typical features of docked BB such as transition fibers, present both in control or *cby*^{1} mutant flies (Fig. 5 C). However, centrioles are present at the tip of the dendrites and apparently show distal projections but are not connected to the membrane (Fig. 5, C and D). This phenotype differs from observations of mutants of genes encoding centriolar proteins, such as *plp*, for which all BBs fail to reach the distal part of the dendrite (Galletta et al., 2014).

Altogether, these results show that Cby and Dila cooperate to build the TZ and recruit most described TZ components in *Drosophila* sensory neurons (Fig. 5 F).

In double *dila*^{81}*; cby*^{1} mutant flies, in addition to strong sensory defects, males are completely sterile. No mature sperm is produced and examination of testes shows that sperm cysts failed to elongate whereas the overall size of the testes is not reduced (Fig. 6 A). EM examination of testes indicates a severe disorganization of sperm cysts (Fig. S3 A). Most axonemes were absent or completely damaged. Because cysts were severely disorganized, we could only count the number of remaining axonemes relative to the number of major mitochondria derivatives. Out of 442 mitochondria, only 5 intact axonemes (1.2%) and 28 recognizable but destroyed axonemes (6.3%; Fig. S3 A) could be identified. These observations indicate a strong genetic interaction between *cby* and *dila* in flagella formation, as we observed only a small fraction (14%) of defective flagellar axonemes in *cby*^{1} mutants (Enjolras et al.,

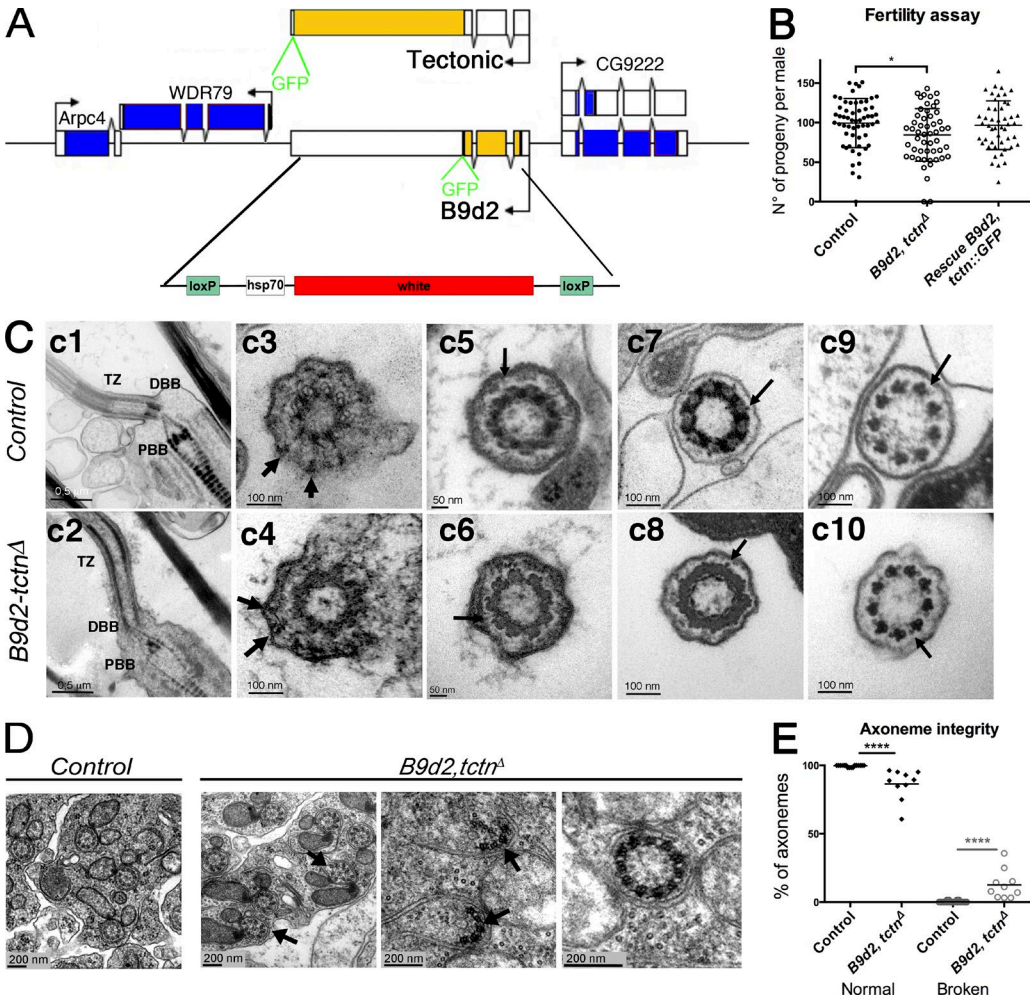

Figure 3. ***B9d2, tctn* mutant flies show only mild fertility defects.** (A) Scheme of the *tctn* and *B9d2* loci. Coding sequences were replaced by the *white* gene using CRISPR/Cas9-induced homologous recombination. (B) Quantification of the number of progeny obtained from individual males (control $n = 58$; *B9d2, tctnΔ* $n = 52$; and rescue $n = 47$) mated with three females. Scattered plot representation with mean and SD; *, $P < 0.05$. (C) Transmission EM analysis of adult antennae chordotonal neurons in control (c1, c3, c5, c7, and c9) or *B9d2, tctnΔ* mutant flies (c2, c4, c6, c8, and c10). (c1 and c2) Longitudinal sections showing no differences in the organization of the BB and TZ region of the cilia. (c3 and c4) Cross sections at the distal part of the BB show transition fibers connecting the BB to the membrane (arrows) in control and *B9d2, tctnΔ* mutant flies. (c5 and c6) Cross sections of the proximal part of the TZ. "Y-like" connectors (arrows) are observed in control and *B9d2, tctnΔ* flies. (c7 and c8) Cross sections of the distal part of the TZ. Small protrusions emanating from the axoneme and directed toward the membrane are observed (arrows) in both control and *B9d2, tctnΔ* flies. (c9 and c10) Cross sections at the proximal part of the sensory cilia show the ninefold symmetry of doublet microtubules and presence of the dynein arms (arrows) in control and *B9d2, tctnΔ* flies. DBB, distal basal body; PBB, proximal basal body; TZ, transition zone. (D) Transmission EM observations of adult testis sections. In mutant testis, a few broken (left and center, black arrows) or odd axonemes (11 doublets on the right) are found compared with control. (E) Quantification of the percentage of abnormal axonemes found per normal ($n = 20$) or mutant ($n = 10$) cysts. Results are presented as a scattered plot with mean and SD; ****, $P < 0.0001$.

2012) and no axonemal defects were described in *dila*^{81} mutants (Ma and Jarman, 2011).

In the absence of both Cby and Dila, we observed that Mks1 and B9d1 (Fig. 6 B) are absent at the tip of BB in *Drosophila* spermatocytes and spermatids. Cep290 was also almost completely lost (Fig. 6 C; greater than sevenfold reduction), whereas no differences in the overall expression levels of Mks1-GFP or Cep290-GFP could be detected in the testes by Western blot (Fig. S3 B). These observations again reveal strong genetic interactions between *dila* and *cby* as MKS proteins and Cep290 are still present in the single *cby* or *dila* mutants and their distribution is only slightly modified (Fig. S4). Only Unc was still present in absence of Cby and Dila (Fig. 6 D). However, Unc distribution was altered, with an expansion of its expression domain, suggesting a defective organization of the ring centriole and membrane cap in the *dila*^{81}*; cby*^{1} double mutant. EM observations of the centrioles in *Drosophila* spermatocytes showed that centrioles did not form a primary cilium-like structure, failed to dock to the plasma membrane, and had an odd orientation inside the cell (Fig. 7 A). No ciliary cap was observed in spermatocytes. Centrioles were apparently normally formed, showing the regular triplet arrangement and the presence of the central tube (Fig. 7 A, a2 and a5, arrow). Strikingly, aberrant microtubule extensions from centrioles were observed (Fig. 7 A, a3, a4, and a6, arrowheads). The absence of docking of the centrioles to the plasma membrane was confirmed by live imaging of centrioles in spermatocytes (Fig. 7 B). In addition, we could confirm the absence of the ciliary cap in spermatids by detecting Rab8, which strongly labels the cap from end of meiosis to late elongation stages (Fig. S3 C). In *dila*^{81}*; cby*^{1} spermatids, Rab8 staining was completely absent from BB distal ends, whereas Rab8 was not affected in *dila*^{81} mutants and present at

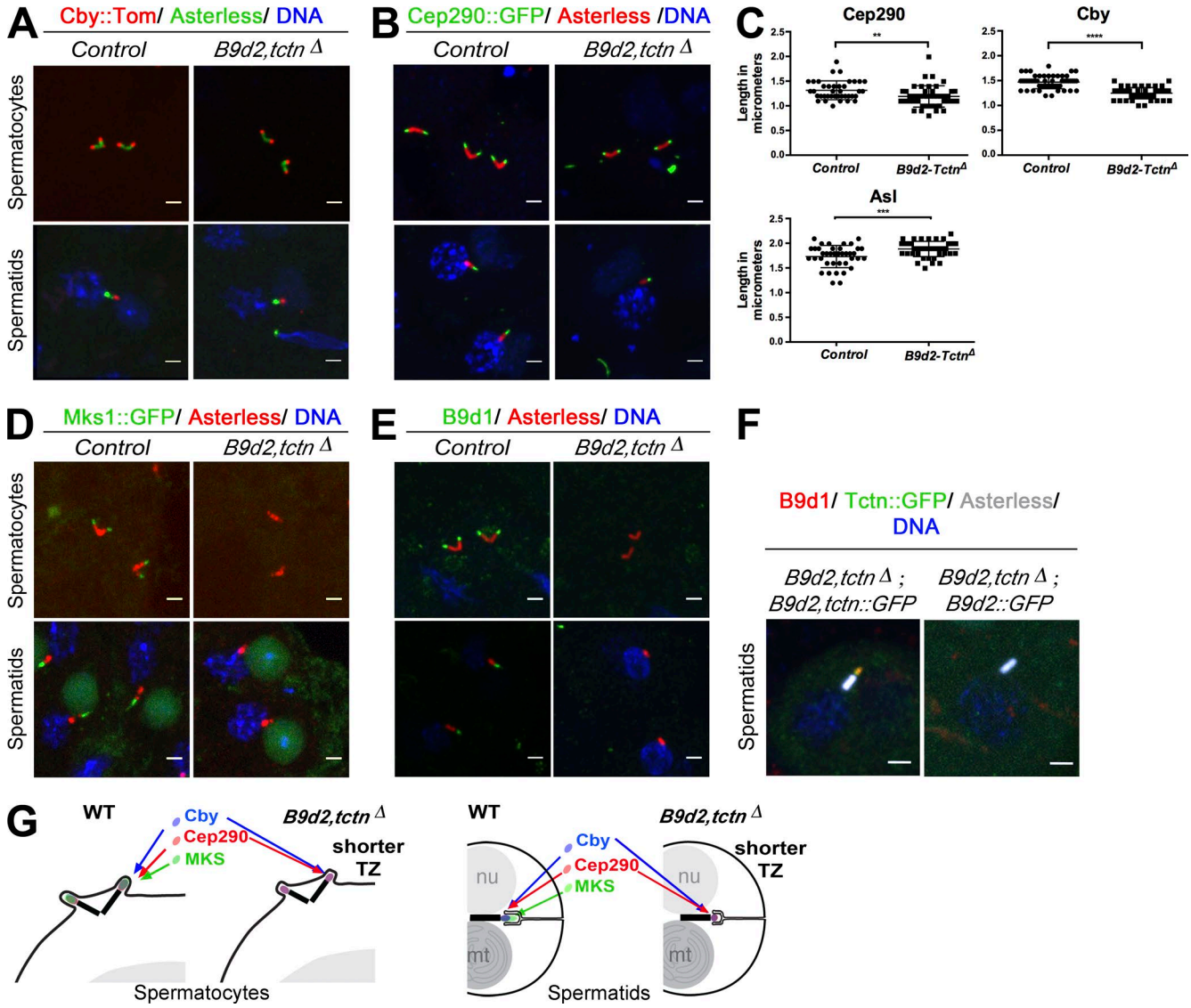

Figure 4. **B9d2 and Tctn are required to assemble the MKS complex and organize the TZ.** (A, B, and D–F). IF analysis of squashed testes. (A and B) Cby and Cep290 localization domains are reduced in length at the TZ of the *B9d2, tctnΔ* mutant spermatocytes or spermatids. (C) Quantification of Cep290, Cby, and centriole lengths in meiosis stage in control or *B9d2, tctnΔ* mutant germ cells. Scattered plots with mean and SD are shown. Cep290 and Asl: control $n = 39$ and *B9d2, tctnΔ* $n = 45$; Cby: control $n = 54$ and *B9d2, tctnΔ* $n = 51$. ****, $P < 0.0001$; **, $P < 0.01$; ***, $P < 0.001$. (D and E) Mks1 and B9d1 are absent from the TZ in *B9d2, tctnΔ* mutant germ cells. (F) B9d1 localization (red) is only rescued when introducing both B9d2 and Tctn, the latter being fused to GFP. No rescue is observed when introducing B9d2 alone. (G) Scheme recapitulating the consequences of *B9d2, tctnΔ* deletion. In the absence of B9d2 and Tctn, the TZ is shorter, as revealed by Cep290 or Cby staining, and all other MKS components are missing. WT, wild type. Bars, 2 µm.

the ciliary cap in a significant fraction (~35%) of the spermatids in *cby*^{1} mutants (Fig. S3 C).

To understand the nature of the aberrant microtubule extensions observed in the double mutants, we labeled cells with markers of tubulin posttranslational modifications. We found that microtubule extensions were acetylated and glutamylated (Fig. 7 C). These modifications are hallmarks of stabilized microtubules but are not restricted to the axoneme. We thus used a reporter marker CG6652 tagged with GFP, which specifically labels the spermatid axoneme in *Drosophila* (this study). Strikingly, whereas this marker only labels the primary cilia in spermatocytes and the ciliary cap in round spermatids (Fig. 7 D), huge extensions are visualized on double mutants, both in spermatocytes and in round spermatids. These extensions are not visible in early spermatocytes and only appear at the time of maturation when centrioles should be docking to the plasma membrane. This shows that premature axoneme elongation is observed in spermatocytes when centrioles fail to dock to the plasma membrane. Altogether, our results demonstrate that Cby and Dila cooperate to build the TZ, which is necessary for the formation of the ciliary cap. In the absence of this ciliary cap, premature axoneme elongation takes place (Fig. 7 E).

Klp59D is present at the sperm ciliary cap and controls timely and proper growth of the axoneme

We hypothesized that premature axoneme elongation could be caused by defective microtubule dynamics at the tips of the centrioles and in particular by defective control of the balance between tubulin polymerization and depolymerization. Several proteins play a role in controlling tubulin assembly.

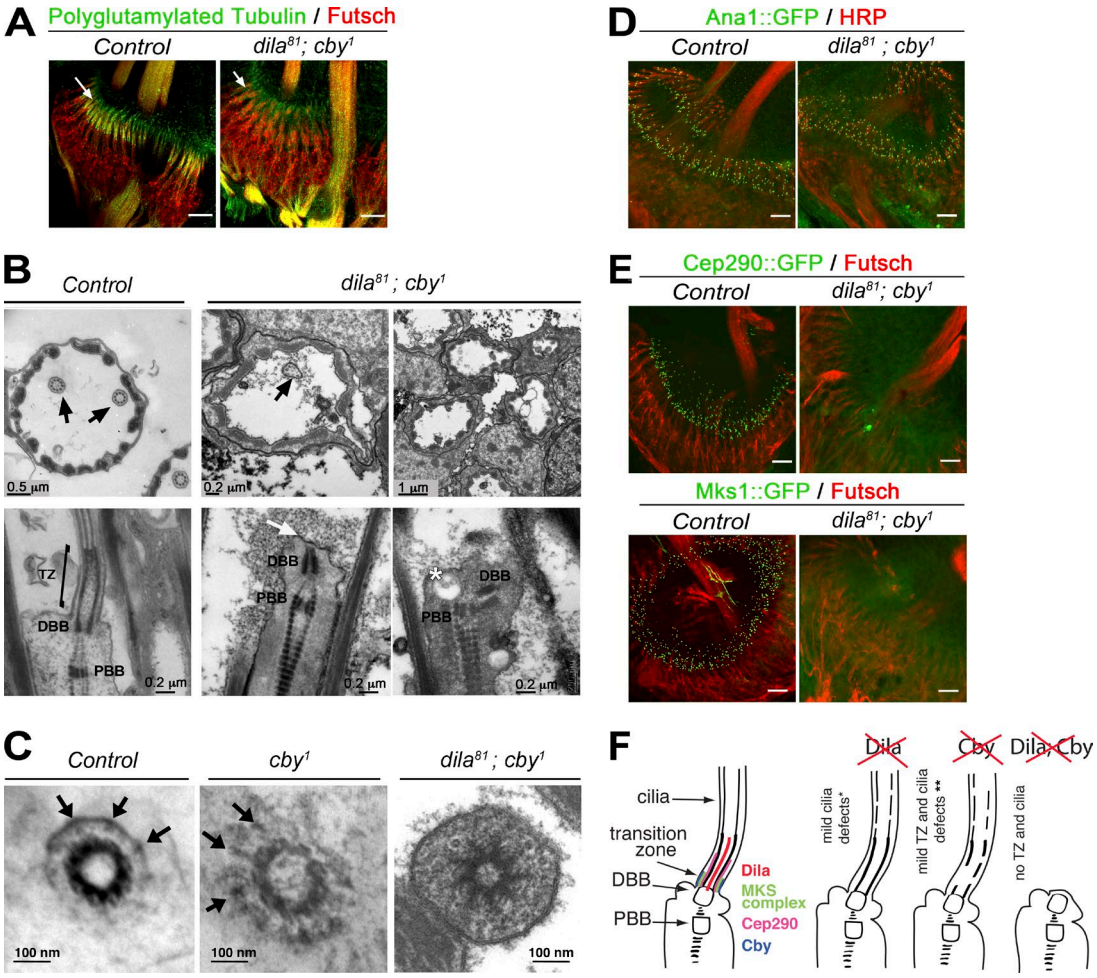

Figure 5. **Cby and Dila cooperate to build the *Drosophila* TZ in sensory cilia.** (A) Whole-mount staining of chordotonal organs of the second antennal segment showing neuronal cell bodies and dendrites (Futsch) and cilia (GT335 antibody). Cilia are missing in *dila*^{81}*; cby*^{1} double mutants. (B) EM analysis of cross section (top) reveals an almost complete absence of cilia, the few remaining ones being severely disorganized compared with control (arrows). On longitudinal sections (bottom), the two BBs (DBB, distal basal body; PBB, proximal basal body) are visible at the tip of the dendrites, but no cilium and TZ are built (white arrow). In some cases, the two BBs are not aligned properly (right), and accumulation of vesicles is seen (asterisk). (C) EM analysis of cross sections at the base of the cilia. Transition fibers (arrows) can be seen connecting the BB to the membrane in control or *cby*^{1} flies. In *dila*^{81}*; cby*^{1}, the BB showed possible distal extensions, but these did not connect the membrane. (D and E) Whole-mount staining of pupae antennae. (D) Centrioles (Ana1::GFP) are still present at the tip of the dendrites (HRP staining) in *dila*^{81}*; cby*^{1} mutants. (E) Cep290 and Mks1 are not recruited at TZ in *dila*^{81}*; cby*^{1} chordotonal organs. (F) Scheme of the defects observed after removing Dila (*, adapted from Ma and Jarman, 2011), Cby (**, adapted from Enjolras et al., 2012), or both (this study). In *dila*^{81} mutant antennae, the TZ is apparently normal by EM. In the *cby*^{1} mutant, the TZ shows incomplete ultrastructural defects. In the double mutant, no TZ is built. Bars, 10 µm (A, D, and E).

In particular, members of the kinesin-13 family of proteins are known to be involved in regulating tubulin depolymerization (Moores and Milligan, 2006). In *Drosophila*, three kinesin-13 family members are present in the genome (Rogers et al., 2004; Hu et al., 2015). Mutations of *Drosophila Klp10A* lead to centriole defects characterized by centriolar fragmentation, increased centriole lengths, and reduced size of primary cilia-like extensions in spermatocytes (Delgehyr et al., 2012; Gottardo et al., 2013), but not to aberrant microtubule extensions. These defects are different from those observed in *dila*^{81}*; cby*^{1} double mutants. Knockdown (KD) of the other two kinesin-13 proteins by RNAi in *Drosophila* showed that only reducing *Klp59D* led to shorten cysts, strikingly similar to cyst phenotypes observed in *dila*^{81}*; cby*^{1} mutant (Noguchi et al., 2011; Fig. S5 A).

We looked for Klp59D distribution using a Klp59D::GFP reporter transgene on live testes cyst preparation. Klp59D::GFP showed a dynamic distribution during germ cell differentiation (Fig. 8 A). In early spermatocytes, Klp59D is present throughout the cytoplasm. During spermatocyte maturation, Klp59D is also enriched at the tips of the centrioles and at their bases in late spermatocytes. Close examination of late spermatocytes show clear enrichment of Klp59D in the ciliary cap protruding from the cell surface (Fig. 8 B). In elongating spermatids, Klp59D is concentrated at the ciliary cap and along the axoneme (Fig. 8 A). We next analyzed the function of *Klp59D* by expressing shRNA in *Drosophila* male germ cells. We observed that the distribution of MKS components, Dila, or Cby was apparently normal in *Klp59D* KD spermatocytes (Fig. 8, C and F), suggesting that Klp59D acts downstream of TZ components. In support of this hypothesis, the amount of Klp59D around centrioles is significantly reduced compared with Asl intensity in the absence of both Dila and Cby (Fig. 8 D). However, Unc distribution was strikingly modified in *Klp59D* KD cells compared with controls (Fig. 8 E). This phenotype is identical to the

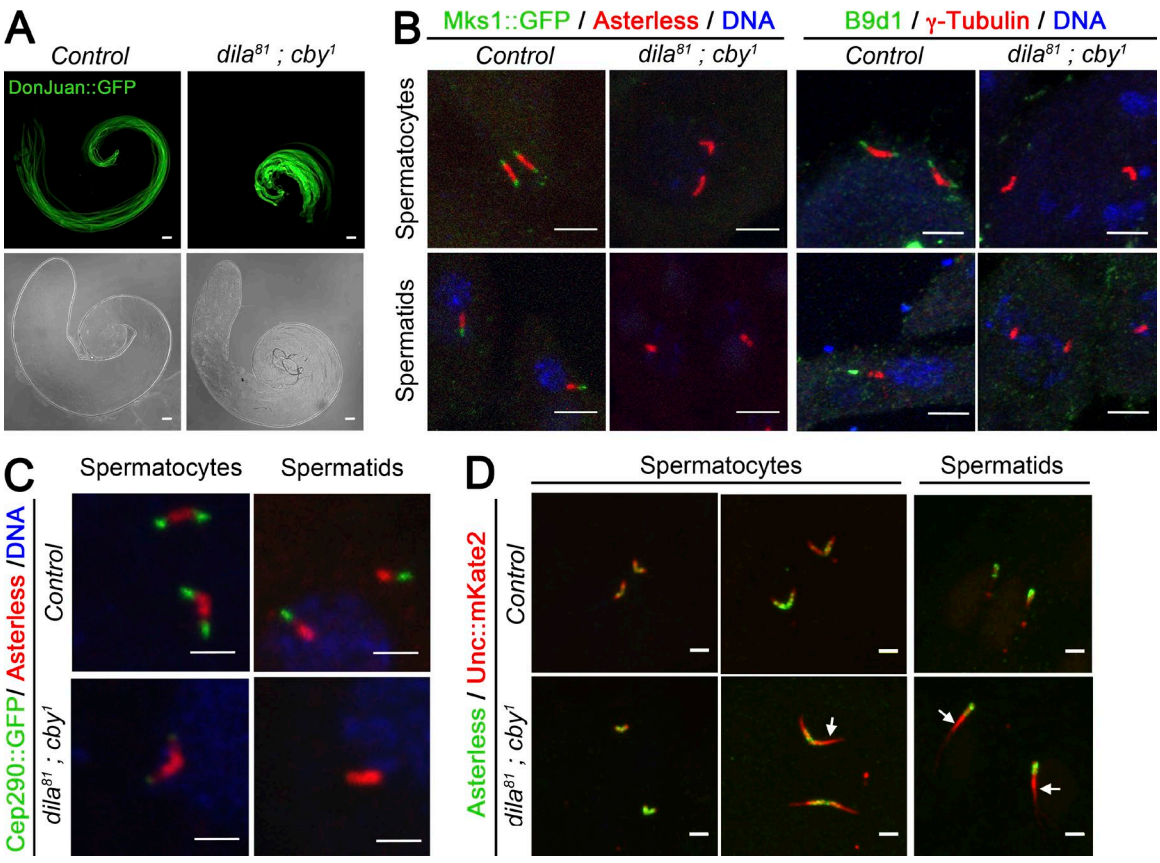

Figure 6. **Cby and Dila cooperate to build the TZ and ciliary cap in male germ cells.** (A) Whole-mount *Drosophila* testis expressing the tagged mitochondria protein DonJuan::GFP observed by bright-field and confocal microscopy. The cysts fail to elongate in *dila*^{81}*; cby*^{1} mutants. (B–D) Confocal imaging of centrioles/BB of squashed testes. (B) Detection of Mks1::GFP or B9d1 (green) and Asterless or γ-tubulin (red), respectively. Mks1 and B9d1 are absent from the tip of the centrioles in spermatocytes and from the tip of BB in spermatids of *dila*^{81}*; cby*^{1} mutants. (C) Cep290::GFP (green) and Asterless (red) staining. Cep290 localization at the tip of the centrioles in spermatocytes and at the tip of BB in spermatids is almost completely lost in *dila*^{81}*; cby*^{1} mutants. (D) No significant differences in Unc::mkate2 localization is observed at early spermatocyte stages. Unc::mKate2 localization is expanded in *dila*^{81}*; cby*^{1} mutants from midspermatocyte stage and in spermatids (arrows). Bars: (A) 50 µm; (B) 5 µm; (C and D) 2 µm.

one observed in *dila*^{81}*; cby*^{1} double mutants and was confirmed with CG6652::GFP labeling, showing huge axonemal extensions on many centrioles in *Klp59D* KD cells (Fig. 8 F). Using a cell membrane marker, we observed that the aberrant axoneme elongation was associated with impaired membrane cap formation in male germ cells (Fig. 8 G). Furthermore, EM observations of spermatocytes showed part of the centrioles with aberrant microtubule elongation and disrupted ciliary cap (Fig. S5 D). These observations indicate that membrane cap formation requires strict control of microtubule elongation. Additionally, EM analysis showed a severe disorganization of spermatid axonemes similar to defects observed in *dila*^{81}*; cby*^{1} mutants. Very few axonemes were apparently normal, and most were missing or broken (Fig. S5, B and C). Altogether, our results show that Klp59D is required for timely control of axonemal growth during male germ cell differentiation. Removal of this protein leads to premature microtubule elongation, axonemal structural defects, and defective ciliary cap formation.

Discussion

Here, we show that TZ assembly in *Drosophila* involves cooperative actions of Cby and Dila, both in sensory neurons and male germ cells. More importantly, we reveal that a timely control of the balance between membrane cap assembly by TZ components and microtubule elongation by kinesin-13 microtubule remodeling is required for proper axoneme formation in *Drosophila* male germ cells.

Flagella assembly in *Drosophila* male germ cells does not rely on IFT, as null mutations in IFT components have no consequences on flagella formation (Han et al., 2003; Sarpal et al., 2003). It is thus considered to be cytosolic, in contrast to the more widely conserved IFT-dependent ciliogenesis, which is said to be compartmentalized (Avidor-Reiss and Leroux, 2015). However, proteins of the ring centriole/TZ such as Unc, Cby, or Cep290 are required to compartmentalize the flagellar growing end in *Drosophila* through the formation of a ciliary cap (Baker et al., 2004; Enjolras et al., 2012; Basiri et al., 2014). The exact function of this ciliary cap is not clear (Avidor-Reiss and Leroux, 2015). It was proposed that the formation of the ciliary cap is associated with the formation of a diffusion barrier, which protects the ciliary end from cytoplasmic proteins (Basiri et al., 2014; Avidor-Reiss et al., 2015). Our results are in agreement with this hypothesis and suggest that the ciliary cap is required to create a specific environment that restricts axonemal growth, as precluding ciliary cap formation in *dila*^{81}*; cby*^{1} mutants leads to aberrant microtubule extensions and unstable axonemes. On the other hand, our results show that unbalanced microtubule growth prevents ciliary cap formation. In agreement with this

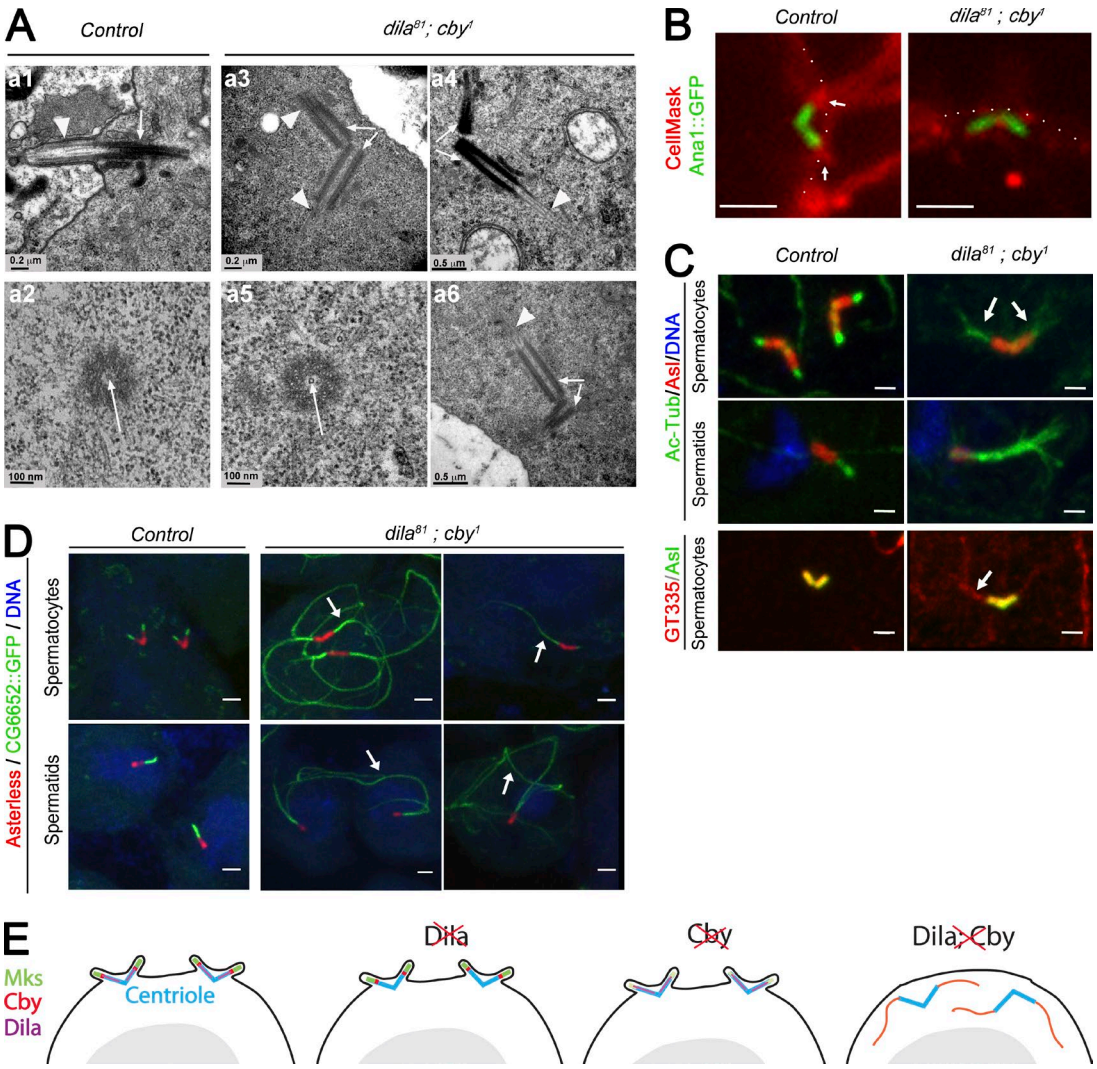

Figure 7. **Aberrant centriolar extension is observed in male germ cells in the absence of the ciliary cap.** (A) Transmission EM analysis of spermatocyte cilia. In control late spermatocytes, centrioles (arrow) are docked to the membrane and cilia (arrowhead) extend at the cell surface. In *dila*^{81}*; cby*^{1} mutants, centrioles (arrows) do not dock to the membrane (a3, a4, and a6) and microtubules extend from the centrioles (arrowheads). The centrioles are apparently unaffected and show the central tubule (a2 and a5, arrows). (B) Live imaging of *Drosophila* spermatocytes labeled with CellMask showing the centrioles (Ana1::GFP) docked to the plasma membrane protruding at the ciliary cap (white arrows) in control cells. The centrioles are present in an inverted orientation under the plasma membrane (dashed line) and not extending a ciliary cap. (C) Squashed spermatocytes and spermatids showing acetylated-tubulin extension (arrows) of the centrioles in double mutants compared with control. Aberrant microtubule extensions are also glutamylated (arrow, GT335 antibody). (D) Confocal imaging of squashed testes showing aberrant extensions of centrioles (arrows) in spermatocytes and spermatids. CG6652::GFP only labels the axoneme and no other microtubules in testes. (E) Scheme summarizing the roles of Cby and Dila in TZ and cilia assembly in *Drosophila* spermatocytes. Removal of Dila does not affect TZ components (see Fig. S3). The absence of Cby mildly affects MKS protein recruitment. Removal of both completely disorganizes TZ assembly and ciliary cap formation. The absence of ciliary cap is associated with aberrant and premature axonemal extension in spermatocytes. Bars, 2 µm (B–D).

conclusion, previous work showed that treatment of spermatocytes with Taxol leads to Unc domain extension, associated with aberrant axoneme elongation and defective ciliary cap formation, when treatment was applied on spermatocytes before BB docking, but not when applied after BB docking (Riparbelli et al., 2013). Therefore, cytosolic ciliogenesis in *Drosophila* is regulated by a precise balance between microtubule extension from the centriole distal end and membrane cap formation.

This mechanism is apparently specific to cytosolic ciliogenesis. In *dila*^{81}*; cby*^{1} sensory cilia, the total absence of the TZ is not associated with aberrant axoneme elongation. This also indicates that centriole docking in this tissue is a prerequisite to elongate the axoneme. Klp59D is not expressed in sensory neurons, and driving Klp59D shRNA expression in sensory neurons did not reveal any sensory defects. These differences could reflect particular properties of centrioles in *Drosophila* spermatocytes. Indeed, all four centrioles convert to BB in spermatocytes, whereas only the mother centriole does so in sensory neurons (Tates, 1971). Therefore, different sets of proteins should be involved in centriole maturation in spermatocytes compared with sensory neurons. Further work will be required to understand molecular differences between sperm and sensory basal bodies.

Another set of observations highlights the particular behavior of spermatocyte centrioles. Mutations in TZ proteins have shown that reducing the length of primary cilia-like/TZ in spermatocytes is associated with an increase in length of the centrioles. This was observed when removing Cep290 (Basiri et al.,

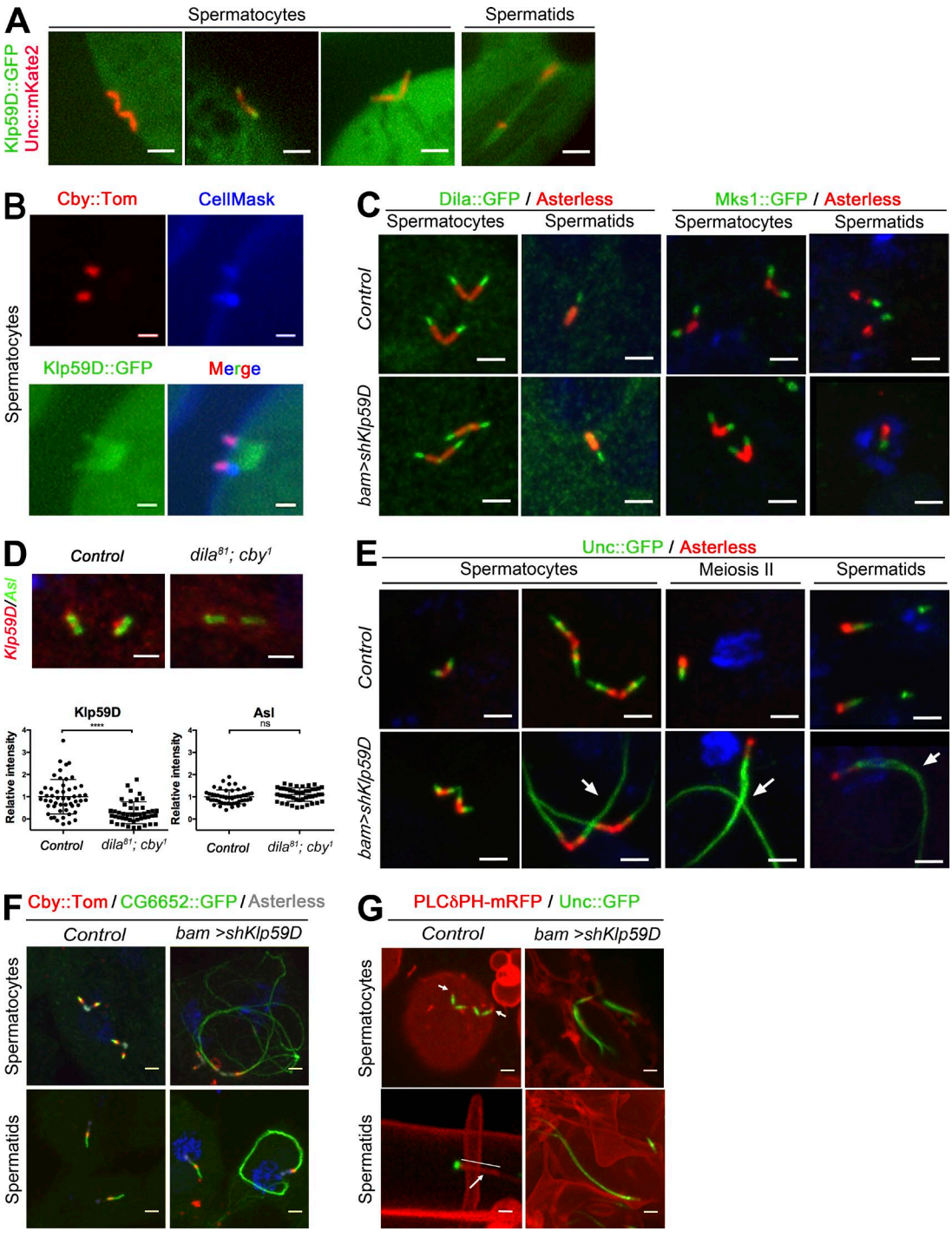

Figure 8. **Klp59D acts downstream of TZ components to regulate axonemal assembly in spermatogenesis.** (A) Live observation of Klp59D::GFP distribution. In spermatocytes, Klp59D is first cytoplasmic and next recruited at centrioles. In elongating spermatids, Klp59D::GFP is present at the tip of the BB and along the axoneme and ciliary cap. (B) Magnification of centrioles and primary cilia in late spermatocytes, showing the localization of Klp59D::GFP in the cilia/TZ extension (labeled with Cby::Tomato) and at the base of the centrioles. (C–E) Confocal imaging of squashed testes. (C) TZ components Dila and Mks1 are recruited normally at centriole tips (Asl antibody) in spermatocytes and spermatids in *Klp59D* KD compared with control testes. (D) Quantification of Klp59D and Asl relative intensities in control or *dila*^{81}*; cby*^{1} spermatocytes. Significant differences are observed for Klp59D. Scattered plots with mean and SD are shown (control $n = 52$; *dila*^{81}*; cby*^{1} $n = 46$). (E) Unc::GFP expression domain is extended in late spermatocytes and spermatids (arrows) in *Klp59D* KD compared with controls. (F) Cby is still present at the tip of centrioles, but huge axonemal extensions are labeled by CG6652::GFP in *Klp59D* KD testes. (G) Live cyst imaging using the membrane PLCδPH-mRFP and Unc::GFP reporters. In control cysts, a membrane cap (arrows, straight line indicating the range of the cap) is present at the tip of centrioles and BBs. In *Klp59D* KD, the membrane cap is absent when aberrant microtubule extensions are observed, as revealed by the extended expression domain of Unc. Bars: (B and D) 1 µm; (A, C, and E–G) 2 µm.

2014), and we made identical observations on *B9d2, tctn*$^{\Delta}$ mutant testes. Thus, reducing ciliary cap extension allows centriole elongation, suggesting a balance in centriolar extension controlled by the TZ. Such a balance was also revealed by removal of Klp10A, which leads to an increase in centriole elongation and in a simultaneous reduction of primary cilia/TZ extension (Gottardo et al., 2013). Hence, the kinesin-13 proteins Klp10A and Klp59D likely play complementary functions at the spermatocyte TZ by restricting, respectively, centriole elongation or TZ elongation.

The function of kinesin-13 family members in ciliogenesis is still unclear and sometimes contradictory. In protozoa, such as *Giardia intestinalis*, *Leishmania*, or *Trypanosoma,* removal of kinesin-13 leads to longer flagella (Blaineau et al., 2007; Dawson et al., 2007; Chan and Ersfeld, 2010) in agreement with a tubulin-depolymerizing function of these proteins. It has also been proposed that kinesin-13 proteins play a role in maintaining a free tubulin pool to promote axoneme assembly (Wang et al., 2013). However, recent studies suggest more complex roles of kinesin-13 members in cilia assembly. In mammals, Kif24 is required to regulate centriole length by interacting with CP110 (Kobayashi et al., 2011). Such a function is also true for Klp10A in *Drosophila* (Delgehyr et al., 2012; Franz et al., 2013). Thus, one possible explanation for the observed phenotype in the *dila*^{81}*; cby*^{1} double mutant would be that CP110 is prematurely removed from centrioles, as Dila and CP110 have strikingly similar localization inside the TZ lumen (this study and Franz et al., 2013, respectively). However, complete removal or overexpression of CP110 in *Drosophila* did not lead to measurable ciliary defects and obviously did not lead to aberrant centriolar extensions in male germ cells (Franz et al., 2013). Therefore, modulation of CP110 activity cannot explain the aberrant axonemal growth observed in the testes in both *dila*^{81}*; cby*^{1} mutants and *Klp59D* KD.

In *Tetrahymena,* kinesin-13 protein was shown to act as an axoneme assembly factor by regulating the levels of tubulin modification and in particular tubulin acetylation inside the cilia (Vasudevan et al., 2015). It is tempting to speculate that Klp59D could play such a function in the ciliary cap of the sperm germ cell. However, it is difficult to test this hypothesis, as quantifications of differences in tubulin modifications inside the ciliary cap by IF are difficult and biochemical quantification of tubulin modifications is limited by the huge amount of nonaxonemal (cytoplasmic) modified microtubules in male germ cells.

Our study reveals both analogies and differences in TZ assembly between *Drosophila* and other organisms. In mammals, MKS proteins play a critical function on TZ assembly and subsequently cilia function as revealed by human ciliopathies, in which these proteins are mutated (Garcia-Gonzalo et al., 2011; Czarnecki and Shah, 2012; Reiter et al., 2012). In *C. elegans*, mutations in the five core members of the MKS complex (Tctn, MKSR-1 [B9d1], MKSR-2 [B9d2], MKS1 [B9d3], and MKS6 [Cc2d2A]; Bialas et al., 2009; Williams et al., 2011; Yee et al., 2015) have no effect on cilia architecture and sensory function. However, functional interactions were revealed between them, as their localization at the TZ is interdependent. In addition, whereas no genetic interactions are revealed when looking at sensory functions, combining mutations in several of these genes led to modified lifespan, suggesting that MKS components cooperate in specific ciliary signaling functions in *C. elegans*. (Bialas et al., 2009). In *Drosophila*, our results indicate that, like in nematodes, the MKS complex has only subtle functions on TZ and cilia assembly and that MKS components exhibit functional interactions, as removing B9d2 and Tctn is sufficient to completely alter the recruitment of the other MKS members. In this context, we do not expect to reveal genetic interactions by combining other mutations in MKS components together with our *B9d2, tctn* mutant. Our observations therefore suggest that the hierarchy and function of MKS components are likely conserved between *C. elegans* and *Drosophila*.

In contrast, strong genetic interactions have been described between MKS and NPHP components in *C. elegans*. In particular, MKS5 (Rpgrip1L or NPHP8 in mammals) acts upstream of all other components to build the TZ (Fig. 1 A), and NPHP4 and 1 interact with MKS complex proteins to organize the TZ (Williams et al., 2011; Sung and Leroux, 2013; Yee et al., 2015). These NPHP members are not conserved in *Drosophila*. Therefore, other proteins should be required to organize the ciliary TZ upstream of the MKS complex in *Drosophila*. Among conserved candidates in other organisms, Cep290 is required to build the TZ in *Drosophila,* but MKS components are still assembled at the TZ in Cep290 mutants (Basiri et al., 2014), thus suggesting that other TZ components act upstream of MKS. Here, we demonstrate that *cby* and *dila* show strong genetic interaction in TZ assembly, whereas mutating each separately only shows moderate effects. These results highlight for the first time the synergistic roles of Cby and Dila in building the TZ.

Cby and Dila are not present in *C. elegans* but are conserved in mammals. In mouse, Cby plays an important role in motile ciliated epithelia, as demonstrated by the severe airway ciliogenesis defects observed in *Cby* knockout mice (Voronina et al., 2009; Burke et al., 2014). In mammalian cells, Cby is also required for primary cilia assembly (Lee et al., 2014). Interestingly, mammalian Cby is required to dock centrioles to the plasma membrane (Voronina et al., 2009; Burke et al., 2014), a function that is only revealed in *Drosophila* by removing both Cby and Dila (Enjolras et al., 2012; this study). Mammalian Cby is required for Rab8-mediated ciliary vesicle assembly (Burke et al., 2014), and we show here that Rab8 recruitment at the ciliary cap is also partially affected in *cby*^{1} mutant flies and strikingly completely abolished in *dila*^{81}*; cby*^{1} double mutants. This suggests a conserved role of Cby in Rab8-associated membrane cap assembly from *Drosophila* to mammals and highlights that Dila is also required for this process in *Drosophila*. In mammals, Azi1 (Dila in *Drosophila*) is a centriolar satellite component required for centriole duplication, but it is also localized at centrioles and is required for cilia assembly (Hall et al., 2013; Villumsen et al., 2013; Chamling et al., 2014). However, its function in TZ assembly has not been investigated. In *Drosophila*, Dila is found restricted to the BB and TZ and is required for cilia assembly, but no specific defects of the TZ were detected in mutant flies (Ma and Jarman, 2011). Thus, our study in *Drosophila* reveals that Dila is also involved in building the TZ but that alternative pathways can compensate for Dila deficiency in TZ assembly. Such compensation mechanisms have also been proposed for Azi1 in mammals (Hall et al., 2013).

In conclusion, our study reveals critical genetic interactions between two yet-unrelated TZ proteins, Cby and Dila. Future work will be required to understand if such interactions are also conserved in mammals. This work also demonstrates that the formation of a ciliary cap is essential to coordinate ciliary assembly during cytosolic ciliogenesis by creating a biochemical environment that controls axonemal microtubule growth.

Materials and methods

Fly stocks and maintenance

The following lines were obtained from Bloomington *Drosophila* Stock Center: vasa::Cas9 (Bl#51323), UAS-Dcr2 (Bl#24648), and Don-Juan::GFP (Bl#5417). The shRNA against Klp59D (v100530) was obtained from the Vienna *Drosophila* Stock Center. The Rab8::YFP strain was described previously (Dunst et al., 2015). The cby^{1} mutant and Cby::GFP and Cby::Tomato transgenes were also previously described (Enjolras et al., 2012). The bam-GAL4::VP16 construct was described previously (Chen and McKearin, 2003). The Unc::GFP transgene was a gift from M. Kernan (State University of New York, Stony Brook, NY; Baker et al., 2004) and Ana1::GFP and Cep290::GFP were gifts from T. Avidor-Reiss (University of Toledo, Toledo, OH; Blachon et al., 2009; Basiri et al., 2014). PLCδPH-mRFP stock was a gift from J. Brill (SickKids, Toronto, Canada; Wei et al., 2008). The $dila^{81}$ mutant was provided by A. Jarman (University of Edinburgh, Edinburgh, Scotland, UK; Ma and Jarman, 2011). The flies were raised on standard media between 21°C and 25°C.

Drosophila reporter gene constructs

pJT61. 6xMycTag-SV40polyA fragment was amplified from pCS2+ nlsMT plasmid (a gift from R. Rupp, Adolf-Buteland Institute, Munich, Germany) and cloned in the XbaI site of the pattB vector (Bischof et al., 2013). EGFP sequence was amplified from pEGFP-N1 plasmid (Takara Bio Inc.) and cloned in the KpnI site of the previous construct, in frame with the 6xMycTag sequence.

pJT108. The Tomato sequence was obtained by PCR on the Zeo-TomatoNT-2 (a gift from R. Basto, Institut Curie, Paris, France) and further cloned in the KpnI site of the pattB plasmid. SV40polyA was amplified from pEGFP-N1 plasmid (Takara Bio Inc.) and cloned in the XbaI site of the previous plasmid.

pJT82. mKate2 and SV40polyA fragments were amplified from pmKate2-N plasmid (Evrogen). The two fragments were further cloned in the XbaI site of the pattB vector.

For each gene, the entire coding and at least 1 kb of upstream regulatory sequences were cloned in frame with GFP in the pJT61 vector or in frame with mKate2 in the pJT82 vector. Integration platforms and primers used were *Mks1::GFP* (89E11 [III]): forward (F)-1, 5′-TAATTCGCGGCCGCCTCTTCGACTTTCTGCTGCA-3′ and reverse (R)-2, 5′-TAATTCGTCGACAAACTCAGCCTGGTAGTATGC-3′; *B9d2::GFP* (68D2 [II]): F-3, 5′-TAATTCGCGGCCGCCAGCTGC ATTATCAAGTACACC-3′ and R-4, 5′-TAATTCCTCGAGCTTGAA CTCCACGCCGTATTC-3′; *tectonic::GFP* (68D2 [II]): F-3 and R-5, 5′-TAATTCCTCGAGGAGGCAAAGTTGCATGGATC-3′; *dila::GFP* (89E11 [III]): F-6, 5′-TAATTCGAATTCCAGCATACCCACTCCGGA TC-3′ and R-7, 5′-TAATTCCTCGAGTTTAACACAATAATCCTT GCG-3′; *Klp59D::GFP* (22A3 [II]): F-8, 5′-TAATTCAGATCTTGT GACTGACATCTCGGTG-3′ and R-9, 5′-TAATTCGCGGCCGCA GCTCGGATTCATCCAGCTCG-3′; *cc2d2a::GFP* (65B2 [III]): F-10, 5′-TAATTCCGGCCGGCCCTGCGAGAATTACCTAG-3′ and R-11, 5′-GAATTACGGCCGCTCCACCAATGGCACCATG-3′; *unc::mKate2* (59D3 [II]): F-12, 5′-TAATTCGCGGCCGCGGAGTACTTC TGCGCCAGG-3′ and R-13, 5′-TAATTCGTCGACCAGGTTTAT GCGTTTCCAG-3′; *CG6652::GFP* (53B2 [II]): F-14, 5′-TAATTC GGATCCAAGCTTGAAGCCCAATTCAA-3′ and R-15, 5′-TAATTC GCGGCCGCAGGTCCTGGCTCTTGTTGTCGT-3′.

For B9d1::Tomato (CG14870), the 2.9 kb BamHI–NotI fragment from the CG14870-6xMycTag reporter plasmid (Enjolras et al., 2012) was subcloned in pJT108 in frame with Tomato and integrated in platform 59D3 (II). All transgenic lines were obtained from BestGene Inc.

Generation of *B9d2, tctn* mutant

The mutant for *B9d2, tctn* (CG42730 and CG42731) was generated by CRISPR/Cas9 catalyzed homologous directed repair (Gratz et al., 2014). Two gRNA were selected using the http://tools.flycrispr.molbio.wisc.edu/targetFinder/ website: 5′-CCACGCAGCAGATACACCTGT CC-3′ and 5′-GTTGCGAGTTGCATAGATGATGG-3′ (protospacer adjacent motifs are underlined). Oligos were phosphorylated by T4PNK (New England Biolabs, Inc.) and annealed. Double-stranded 5′gRNA and 3′gRNA were cloned in the BbsI site of pBFv-U6.2 or pBFv-U6.2B vectors, respectively (Kondo and Ueda, 2013). 5′gRNA was further subcloned in the EcoRI–NotI sites of pBFv-U6.2B to express the two gRNAs from one vector.

The 5′ and 3′ homology arms were amplified by PCR and cloned, respectively, into the EcoRI–NdeI and SpeI–XhoI sites of pRK2 plasmid (Huang et al., 2008). The two vectors (gRNAs and homology arms) were injected into Vasa::Cas9 embryos. Flies were crossed to w; Bl/CyO virgin females and the offspring were screened for red-eyed flies. Homologous recombination was checked by PCR.

Immunofluorescence

***Drosophila* testes squashes.** For PFA fixation, testes from young adult flies or pupae were dissected in 1× PBS, fixed for 15 min in 1× PBS/4% PFA, squashed between the coverslip and slide, and frozen in liquid nitrogen. The coverslip was removed, and the slide was soaked for a few seconds in ethanol 100% at −20°C. Testes were permeabilized for 25 min in 1× PBS/0.1% Triton X-100 (PBT) and blocked for 1 h in PBT/3% BSA/5% NGS. Primary antibodies were incubated in blocking solution overnight at 4°C or 1 h at RT. For Klp59D staining, testes were first kept in 1× PBS for 1 h at 4°C to depolymerize cytoplasmic microtubules, followed by fixation.

Methanol fixation. Testes from young adult flies or pupae were dissected in PBS, opened with a tungsten needle on a slide, and squashed. Slide was frozen in liquid nitrogen and coverslip removed. Samples were fixed 10 min in methanol 100% at −20°C, washed in PBS and blocked for 1 h in PBS/0.1% BSA. Primary antibodies were incubated in blocking solution overnight at 4°C or 1 h at RT (4 h for acetylated tubulin). For acetylated tubulin, testes were kept in PBS for 1 h at 4°C to depolymerize cytoplasmic microtubules before fixation.

For both fixations, fixed testes were washed in PBS and incubated for 1 h in secondary antibodies diluted in PBS. Slides were washed in PBS, incubated in Hoechst 1/1,000 for 15 min at RT, washed in PBS, and rinsed in ultrapure water. Slides were mounted using Dako or Vectashield.

Antennae were processed as previously described (Vieillard et al., 2015). In brief, *Drosophila* heads from 38- to 45-h pupae were dissected in PBS, fixed for 1 h in PBS/4% PFA, and washed in PBS. Antennae were blocked for 1 h in PBS/0.3% Triton X-100/3% BSA/5% NGS and incubated in primary antibodies diluted in blocking solution for 48 h at 4°C. Samples were washed three times in PBS and incubated in secondary antibodies diluted in PBS for 48 h at 4°C. Antennae were washed three times in PBS and mounted in Vectashield.

Antibodies

The antibodies used were the following: mouse anti-Futsch (1/1,000 DSHB = 22c10), mouse anti–acetylated tubulin (1/100, clone 6-11B-1; Sigma-Aldrich), mouse anti–γ-tubulin (1/500; Sigma-Aldrich), mouse anti–polyglutamylated tubulin antibody (1/500, GT335; Enzo Life Sciences), rabbit anti-HRP (1/500; Jackson ImmunoResearch Laboratories, Inc.), rabbit anti-GFP (1/1,000; Abcam), rabbit anti-DsRed (1/2,500; Takara Bio Inc.), guinea pig anti-Asterless (1/45,000; gift from G. Rogers, University of Arizona, Tuscon, AZ; Klebba et al., 2013), rabbit anti-plp (1/1,000; provided by R. Basto, Insitut Curie, Paris, France; Martinez-Campos et al., 2004), mouse anti-Rab8 (1/500;

BD), and rabbit anti-Klp59D (1/1,000; provided by O. Blard and K. Rogowski, Institut de Géntétique Humaine, Montpellier, France). Generation of B9d1 (CG14870) antibody was performed by Eurogentec by immunization of guinea pigs with the following two peptides: PGNEETTPPHEKHKQ and SAKESVPNAMDAKAT. Crude serum was used at 1/2,500 dilution.

The following secondary antibodies were used (all at 1/1,000 dilution): goat anti–mouse Alexa Fluor 488 or Alexa Fluor 594, goat anti–rabbit Alexa Fluor 488 or Alexa Fluor 647, donkey anti–rabbit Alexa Fluor 568, goat anti–guinea pig Alexa Fluor 488 or Alexa Fluor 594 (Invitrogen), and donkey anti–guinea pig Alexa Fluor 647 (Jackson ImmunoResearch Laboratories, Inc.).

Confocal microscopy

All acquisitions were performed at RT. Most slides were imaged using an IX83 microscope (Olympus) equipped with an iXon Ultra 888 EMC DD camera (Andor Technology) and IQ3 software (Andor Technology). A Plan-Apochromat N 60× 1.42 NA objective (Olympus) was used for all acquisitions. Some slides were imaged using an SP5X confocal laser scanning microscope (Leica Biosystems) equipped with the Application Suite software (Leica Biosystems). An HCX Plan-Apochromat CS 63× 1.4 NA objective (Leica Biosystems) was used for all acquisitions. Acquisition of Klp59D KD whole-mount testes slides was made using an epifluorescence axioscope Z1 imager (ZEISS) with an EC Plan-Neofluar 10×/0.3 Ph1 objective (ZEISS), photometrics CoolSNAP MYO camera (Photometrics), and Metavue 7.8.0.0 software. All images were processed with ImageJ. Figures were created with Adobe Photoshop CS5. Unless stated in the figure legends, only contrasts and offset were adjusted.

3D-SIM

Squashes were performed on a 12-mm-diameter round coverslip with a 44 × 60-mm overlaying coverslip. Immunofluorescence protocols were the same as in the Immunofluorescence section using either PFA or methanol fixation. Images were acquired using an Elyra PS.1 system (ZEISS) equipped with a PCO edge 5.5 camera and ZEN 2012 SP2 software (black edition). The objective used for all acquisitions is a Plan-Apochromat 63× 1.4 NA.

Live imaging

Testes of young adults or pupae were dissected in PBS at room temperature, placed in a drop of PBS or PBS/0.5% FCS on glass-bottom poly-lysine–coated (Sigma-Aldrich) Petri dishes (Will-Co). Cells were pulled out of the testes using thinned capillaries and left to attach for 5–15 min. For some experiments, membranes were labeled using CellMask Deep Red Plasma membrane stain (Invitrogen) diluted at 1/50 in a drop of Sang and Shields M3 Insect Medium (Sigma-Aldrich).

EM

Samples were processed as previously described (Enjolras et al., 2012; Vieillard et al., 2015). Antennae or testes were collected in PBS and fixed in 2% glutaraldehyde, 0.5% PFA, and 0.1 M sodium cacodylate, pH 7.4, for 48 h at 4°C. Samples were rinsed in 0.15 M sodium cacodylate, pH 7.4, and postfixed in 1% OsO4 (4 h for antennae and 1 h for testes). Samples were dehydrated through ethanol series and propylene oxide. Samples were substituted in 3 vol propylene oxide/1 vol resin (2 × 30 min), 1 vol propylene oxide/1 vol resin (2 × 30 min), and then 1 vol propylene oxide/3 vol resin (2 × 30 min) and finally embedded in epon medium (Fluka). Ultrathin sections were cut on an ultramicrotome (UC7; Leica Biosystems) and contrasted manually in methanol/uranyl acetate 7% and aqueous lead citrate. Contrasted sections were observed on a transmission EM (CM120; Philips) at 120 kV. Images were acquired with a 2k × 2k digital camera (ORIUS 200; Gatan) and digital micrograph software and processed with Photoshop CS5.

IF quantification

Quantifications of centriole and TZ lengths were performed on sum projections of confocal stacks made with identical settings in control or mutant situation, such to avoid saturated signal. The intensity profile along the centriole or TZ was plotted. Length was measured between the first pixel and the last pixel above the background threshold. Quantification of Klp59D and Cep290 intensities was performed using ImageJ and by measuring the sum of pixel intensity in a defined region encompassing the centrioles. Background intensity was subtracted by measuring the sum of pixel intensity in an adjacent region of the same area next to centrioles. Statistical analyses and graphs were made using Prism 7 software.

Statistics

Quantification results are represented as scatter plots with the mean and SD on all figures. Statistical significance was determined by a two-tailed unpaired Student's *t* test (Prism 6 software; ns, $P > 0.05$; *, $P \leq 0.05$; **, $P \leq 0.01$; ***, $P \leq 0.001$; ****, $P \leq 0.0001$).

Fertility test

1- or 2-d-old males were crossed individually with three w^{1118} virgin females. After 5 d, crosses with at least one dead fly were eliminated from the test. Mated flies were discarded from conserved crosses. All flies that hatched out from the crosses were counted.

Western blot

Proteins were extracted from 48-h pupae (15) testes. Fusion proteins were revealed using a rabbit anti-GFP antibody (1/2,500; Abcam).

Online supplemental material

Fig. S1 shows the localization of MKS components in wild-type or *B9d2, tctnΔ* mutant *Drosophila* antennae. Fig. S2 shows the dynamics of TZ components in the male germ cells. Fig. S3 completes the phenotypic description of $dila^{81}$; cby^{1} mutant germ cells, including transmission EM analysis, Rab8 expression, and MKS1 or Cep290 expression levels. Fig. S4 shows IF analysis and quantification of MKS and Cep290 components in cby^{1} or $dila^{81}$ mutant male germ cells. Fig. S5 completes the phenotypic description of Klp59D KD testes, including EM observations. Online supplemental material is available at http://www.jcb.org/cgi/content/full/jcb.201603086/DC1.

Acknowledgments

We thank R. Basto and M. Delattre for helpful discussions. We are grateful to A. Jarman for sharing the $dila^{81}$ mutant. We thank J. Brill for the PLCδPH-mRFP *Drosophila* stock, T. Avidor-Reiss for the Ana1::GFP and Cep290::GFP *Drosophila* stocks, and K. Rogowski and O. Blard for the unpublished Klp59D antibody. Many thanks to T. Noguchi for training M. Paschaki in germ cyst cultures and to P. Thérond for sharing unpublished observations. We thank C. Maire for her excellent technical support and I. Kimura for help with the *Drosophila* husbandry. We thank C. Chamot, C. Lyonnet (PLATIM), C. Vanbelle, and A. Bouchardon (Ciqle) for help in imaging acquisition. EM observations were performed at the CTμ (University Lyon 1).

This work was supported by grants from the Fondation pour la Recherche Médicale (DEQ20131029168) and the Agence National de la Recherche (Obeli-X). J. Vieillard and C. Augière are supported by a PhD fellowship from the University of Lyon 1. M. Paschaki was

supported by a fellowship from the groupements de recherche Centre National de la Recherche Scientifique "cil" and by the Bonus Qualité Recherche from the University of Lyon 1.

The authors declare no competing financial interests.

Submitted: 24 March 2016
Accepted: 26 August 2016

References

Avidor-Reiss, T., and M.R. Leroux. 2015. Shared and distinct mechanisms of compartmentalized and cytosolic ciliogenesis. *Curr. Biol.* 25:R1143–R1150. http://dx.doi.org/10.1016/j.cub.2015.11.001

Avidor-Reiss, T., A. Khire, E.L. Fishman, and K.H. Jo. 2015. Atypical centrioles during sexual reproduction. *Front. Cell Dev. Biol.* 3:21. http://dx.doi.org/10.3389/fcell.2015.00021

Badano, J.L., N. Mitsuma, P.L. Beales, and N. Katsanis. 2006. The ciliopathies: an emerging class of human genetic disorders. *Annu. Rev. Genomics Hum. Genet.* 7:125–148. http://dx.doi.org/10.1146/annurev.genom.7.080505.115610

Baker, K., and P.L. Beales. 2009. Making sense of cilia in disease: the human ciliopathies. *Am. J. Med. Genet. C. Semin. Med. Genet.* 151C:281–295. http://dx.doi.org/10.1002/ajmg.c.30231

Baker, J.D., S. Adhikarakunnathu, and M.J. Kernan. 2004. Mechanosensory-defective, male-sterile unc mutants identify a novel basal body protein required for ciliogenesis in *Drosophila*. *Development.* 131:3411–3422. http://dx.doi.org/10.1242/dev.01229

Barker, A.R., K.S. Renzaglia, K. Fry, and H.R. Dawe. 2014. Bioinformatic analysis of ciliary transition zone proteins reveals insights into the evolution of ciliopathy networks. *BMC Genomics.* 15:531. http://dx.doi.org/10.1186/1471-2164-15-531

Basiri, M.L., A. Ha, A. Chadha, N.M. Clark, A. Polyanovsky, B. Cook, and T. Avidor-Reiss. 2014. A migrating ciliary gate compartmentalizes the site of axoneme assembly in *Drosophila* spermatids. *Curr. Biol.* 24:2622–2631. http://dx.doi.org/10.1016/j.cub.2014.09.047

Bialas, N.J., P.N. Inglis, C. Li, J.F. Robinson, J.D.K. Parker, M.P. Healey, E.E. Davis, C.D. Inglis, T. Toivonen, D.C. Cottell, et al. 2009. Functional interactions between the ciliopathy-associated Meckel syndrome 1 (MKS1) protein and two novel MKS1-related (MKSR) proteins. *J. Cell Sci.* 122:611–624. http://dx.doi.org/10.1242/jcs.028621

Bischof, J., M. Björklund, E. Furger, C. Schertel, J. Taipale, and K. Basler. 2013. A versatile platform for creating a comprehensive UAS-ORFeome library in *Drosophila*. *Development.* 140:2434–2442. http://dx.doi.org/10.1242/dev.088757

Blachon, S., X. Cai, K.A. Roberts, K. Yang, A. Polyanovsky, A. Church, and T. Avidor-Reiss. 2009. A proximal centriole-like structure is present in *Drosophila* spermatids and can serve as a model to study centriole duplication. *Genetics.* 182:133–144. http://dx.doi.org/10.1534/genetics.109.101709

Blaineau, C., M. Tessier, P. Dubessay, L. Tasse, L. Crobu, M. Pagès, and P. Bastien. 2007. A novel microtubule-depolymerizing kinesin involved in length control of a eukaryotic flagellum. *Curr. Biol.* 17:778–782. http://dx.doi.org/10.1016/j.cub.2007.03.048

Brown, J.M., and G.B. Witman. 2014. Cilia and diseases. *Bioscience.* 64:1126–1137. http://dx.doi.org/10.1093/biosci/biu174

Burke, M.C., F.-Q. Li, B. Cyge, T. Arashiro, H.M. Brechbuhl, X. Chen, S.S. Siller, M.A. Weiss, C.B. O'Connell, D. Love, et al. 2014. Chibby promotes ciliary vesicle formation and basal body docking during airway cell differentiation. *J. Cell Biol.* 207:123–137. http://dx.doi.org/10.1083/jcb.201406140

Carvalho-Santos, Z., P. Machado, I. Alvarez-Martins, S.M. Gouveia, S.C. Jana, P. Duarte, T. Amado, P. Branco, M.C. Freitas, S.T.N. Silva, et al. 2012. BLD10/CEP135 is a microtubule-associated protein that controls the formation of the flagellum central microtubule pair. *Dev. Cell.* 23:412–424. http://dx.doi.org/10.1016/j.devcel.2012.06.001

Chamling, X., S. Seo, C.C. Searby, G. Kim, D.C. Slusarski, and V.C. Sheffield. 2014. The centriolar satellite protein AZI1 interacts with BBS4 and regulates ciliary trafficking of the BBSome. *PLoS Genet.* 10:e1004083. http://dx.doi.org/10.1371/journal.pgen.1004083

Chan, K.Y., and K. Ersfeld. 2010. The role of the Kinesin-13 family protein TbKif13-2 in flagellar length control of *Trypanosoma brucei*. *Mol. Biochem. Parasitol.* 174:137–140. http://dx.doi.org/10.1016/j.molbiopara.2010.08.001

Chen, D., and D.M. McKearin. 2003. A discrete transcriptional silencer in the bam gene determines asymmetric division of the *Drosophila* germline stem cell. *Development.* 130:1159–1170. http://dx.doi.org/10.1242/dev.00325

Chih, B., P. Liu, Y. Chinn, C. Chalouni, L.G. Komuves, P.E. Hass, W. Sandoval, and A.S. Peterson. 2011. A ciliopathy complex at the transition zone protects the cilia as a privileged membrane domain. *Nat. Cell Biol.* 14:61–72. http://dx.doi.org/10.1038/ncb2410

Czarnecki, P.G., and J.V. Shah. 2012. The ciliary transition zone: from morphology and molecules to medicine. *Trends Cell Biol.* 22:201–210. http://dx.doi.org/10.1016/j.tcb.2012.02.001

Dawson, S.C., M.S. Sagolla, J.J. Mancuso, D.J. Woessner, S.A. House, L. Fritz-Laylin, and W.Z. Cande. 2007. Kinesin-13 regulates flagellar, interphase, and mitotic microtubule dynamics in *Giardia intestinalis*. *Eukaryot. Cell.* 6:2354–2364. http://dx.doi.org/10.1128/EC.00128-07

Delgehyr, N., H. Rangone, J. Fu, G. Mao, B. Tom, M.G. Riparbelli, G. Callaini, and D.M. Glover. 2012. Klp10A, a microtubule-depolymerizing kinesin-13, cooperates with CP110 to control *Drosophila* centriole length. *Curr. Biol.* 22:502–509. http://dx.doi.org/10.1016/j.cub.2012.01.046

Dunst, S., T. Kazimiers, F. von Zadow, H. Jambor, A. Sagner, B. Brankatschk, A. Mahmoud, S. Spannl, P. Tomancak, S. Eaton, and M. Brankatschk. 2015. Endogenously tagged rab proteins: a resource to study membrane trafficking in *Drosophila*. *Dev. Cell.* 33:351–365. http://dx.doi.org/10.1016/j.devcel.2015.03.022

Enjolras, C., J. Thomas, B. Chhin, E. Cortier, J.L. Duteyrat, F. Soulavie, M.J. Kernan, A. Laurençon, and B. Durand. 2012. *Drosophila* chibby is required for basal body formation and ciliogenesis but not for Wg signaling. *J. Cell Biol.* 197:313–325. http://dx.doi.org/10.1083/jcb.201109148

Fabian, L., and J.A. Brill. 2012. *Drosophila* spermiogenesis: big things come from little packages. *Spermatogenesis.* 2:197–212. http://dx.doi.org/10.4161/spmg.21798

Franz, A., H. Roque, S. Saurya, J. Dobbelaere, and J.W. Raff. 2013. CP110 exhibits novel regulatory activities during centriole assembly in Drosophila. *J. Cell Biol.* 203:785–799. http://dx.doi.org/10.1083/jcb.201305109

Galletta, B.J., R.X. Guillen, C.J. Fagerstrom, C.W. Brownlee, D.A. Lerit, T.L. Megraw, G.C. Rogers, and N.M. Rusan. 2014. *Drosophila* pericentrin requires interaction with calmodulin for its function at centrosomes and neuronal basal bodies but not at sperm basal bodies. *Mol. Biol. Cell.* 25:2682–2694. http://dx.doi.org/10.1091/mbc.E13-10-0617

Garcia-Gonzalo, F.R., K.C. Corbit, M.S. Sirerol-Piquer, G. Ramaswami, E.A. Otto, T.R. Noriega, A.D. Seol, J.F. Robinson, C.L. Bennett, D.J. Josifova, et al. 2011. A transition zone complex regulates mammalian ciliogenesis and ciliary membrane composition. *Nat. Genet.* 43:776–784. http://dx.doi.org/10.1038/ng.891

Gogendeau, D., and R. Basto. 2010. Centrioles in flies: the exception to the rule? *Semin. Cell Dev. Biol.* 21:163–173. http://dx.doi.org/10.1016/j.semcdb.2009.07.001

Gottardo, M., G. Callaini, and M.G. Riparbelli. 2013. The cilium-like region of the *Drosophila* spermatocyte: an emerging flagellum? *J. Cell Sci.* 126:5441–5452. http://dx.doi.org/10.1242/jcs.136523

Gratz, S.J., F.P. Ukken, C.D. Rubinstein, G. Thiede, L.K. Donohue, A.M. Cummings, and K.M. O'Connor-Giles. 2014. Highly specific and efficient CRISPR/Cas9-catalyzed homology-directed repair in *Drosophila*. *Genetics.* 196:961–971. http://dx.doi.org/10.1534/genetics.113.160713

Hall, E.A., M. Keighren, M.J. Ford, T. Davey, A.P. Jarman, L.B. Smith, I.J. Jackson, and P. Mill. 2013. Acute versus chronic loss of mammalian Azi1/Cep131 results in distinct ciliary phenotypes. *PLoS Genet.* 9:e1003928. http://dx.doi.org/10.1371/journal.pgen.1003928

Han, Y.-G., B.H. Kwok, and M.J. Kernan. 2003. Intraflagellar transport is required in *Drosophila* to differentiate sensory cilia but not sperm. *Curr. Biol.* 13:1679–1686. http://dx.doi.org/10.1016/j.cub.2003.08.034

Hu, Q., and W.J. Nelson. 2011. Ciliary diffusion barrier: the gatekeeper for the primary cilium compartment. *Cytoskeleton (Hoboken).* 68:313–324. http://dx.doi.org/10.1002/cm.20514

Hu, Z., Y. Liang, D. Meng, L. Wang, and J. Pan. 2015. Microtubule-depolymerizing kinesins in the regulation of assembly, disassembly, and length of cilia and flagella. *In* International Review of Cell and Molecular Biology. K.W. Jeon, editor. Elsevier, New York. 241–265.

Huang, J., W. Zhou, A.M. Watson, Y.-N. Jan, and Y. Hong. 2008. Efficient ends-out gene targeting in *Drosophila*. *Genetics.* 180:703–707. http://dx.doi.org/10.1534/genetics.108.090563

Jana, S.C., M. Bettencourt-Dias, B. Durand, and T.L. Megraw. 2016. *Drosophila melanogaster* as a model for basal body research. *Cilia.* 5:22. PudbMedhttp://dx.doi.org/10.1186/s13630-016-0041-5

Jensen, V.L., C. Li, R.V. Bowie, L. Clarke, S. Mohan, O.E. Blacque, and M.R. Leroux. 2015. Formation of the transition zone by Mks5/Rpgrip1L establishes a ciliary zone of exclusion (CIZE) that compartmentalises ciliary signalling proteins and controls PIP2 ciliary abundance. *EMBO J.* 34:2537–2556. http://dx.doi.org/10.15252/embj.201488044

Klebba, J.E., D.W. Buster, A.L. Nguyen, S. Swatkoski, M. Gucek, N.M. Rusan, and G.C. Rogers. 2013. Polo-like kinase 4 autodestructs by generating its Slimb-binding phosphodegron. *Curr. Biol.* 23:2255–2261. http://dx.doi.org/10.1016/j.cub.2013.09.019

Kobayashi, T., W.Y. Tsang, J. Li, W. Lane, and B.D. Dynlacht. 2011. Centriolar kinesin Kif24 interacts with CP110 to remodel microtubules and regulate ciliogenesis. *Cell.* 145:914–925. http://dx.doi.org/10.1016/j.cell.2011.04.028

Kondo, S., and R. Ueda. 2013. Highly improved gene targeting by germline-specific Cas9 expression in *Drosophila*. *Genetics.* 195:715–721. http://dx.doi.org/10.1534/genetics.113.156737

Lee, Y.L., J. Santé, C.J. Comerci, B. Cyge, L.F. Menezes, F.-Q. Li, G.G. Germino, W.E. Moerner, K. Takemaru, and T. Stearns. 2014. Cby1 promotes Ahi1 recruitment to a ring-shaped domain at the centriole-cilium interface and facilitates proper cilium formation and function. *Mol. Biol. Cell.* 25:2919–2933. http://dx.doi.org/10.1091/mbc.E14-02-0735

Li, C., V.L. Jensen, K. Park, J. Kennedy, F.R. Garcia-Gonzalo, M. Romani, R. De Mori, A.-L. Bruel, D. Gaillard, B. Doray, et al. 2016. MKS5 and CEP290 dependent assembly pathway of the ciliary transition zone. *PLoS Biol.* 14:e1002416. http://dx.doi.org/10.1371/journal.pbio.1002416

Ma, L., and A.P. Jarman. 2011. Dilatory is a *Drosophila* protein related to AZI1 (CEP131) that is located at the ciliary base and required for cilium formation. *J. Cell Sci.* 124:2622–2630. http://dx.doi.org/10.1242/jcs.084798

Martinez-Campos, M., R. Basto, J. Baker, M. Kernan, and J.W. Raff. 2004. The *Drosophila* pericentrin-like protein is essential for cilia/flagella function, but appears to be dispensable for mitosis. *J. Cell Biol.* 165:673–683. http://dx.doi.org/10.1083/jcb.200402130

Moores, C.A., and R.A. Milligan. 2006. Lucky 13-microtubule depolymerisation by kinesin-13 motors. *J. Cell Sci.* 119:3905–3913. http://dx.doi.org/10.1242/jcs.03224

Noguchi, T., M. Koizumi, and S. Hayashi. 2011. Sustained elongation of sperm tail promoted by local remodeling of giant mitochondria in *Drosophila*. *Curr. Biol.* 21:805–814. http://dx.doi.org/10.1016/j.cub.2011.04.016

Phillips, D.M. 1970. Insect sperm: their structure and morphogenesis. *J. Cell Biol.* 44:243–277. http://dx.doi.org/10.1083/jcb.44.2.243

Reiter, J.F., O.E. Blacque, and M.R. Leroux. 2012. The base of the cilium: roles for transition fibres and the transition zone in ciliary formation, maintenance and compartmentalization. *EMBO Rep.* 13:608–618. http://dx.doi.org/10.1038/embor.2012.73

Riparbelli, M.G., G. Callaini, and T.L. Megraw. 2012. Assembly and persistence of primary cilia in dividing *Drosophila* spermatocytes. *Dev. Cell.* 23:425–432. http://dx.doi.org/10.1016/j.devcel.2012.05.024

Riparbelli, M.G., O.A. Cabrera, G. Callaini, and T.L. Megraw. 2013. Unique properties of *Drosophila* spermatocyte primary cilia. *Biol. Open.* 2:1137–1147. http://dx.doi.org/10.1242/bio.20135355

Rogers, G.C., S.L. Rogers, T.A. Schwimmer, S.C. Ems-McClung, C.E. Walczak, R.D. Vale, J.M. Scholey, and D.J. Sharp. 2004. Two mitotic kinesins cooperate to drive sister chromatid separation during anaphase. *Nature.* 427:364–370. http://dx.doi.org/10.1038/nature02256

Sang, L., J.J. Miller, K.C. Corbit, R.H. Giles, M.J. Brauer, E.A. Otto, L.M. Baye, X. Wen, S.J. Scales, M. Kwong, et al. 2011. Mapping the NPHP-JBTS-MKS protein network reveals ciliopathy disease genes and pathways. *Cell.* 145:513–528. http://dx.doi.org/10.1016/j.cell.2011.04.019

Sarpal, R., S.V. Todi, E. Sivan-Loukianova, S. Shirolikar, N. Subramanian, E.C. Raff, J.W. Erickson, K. Ray, and D.F. Eberl. 2003. *Drosophila* KAP interacts with the kinesin II motor subunit KLP64D to assemble chordotonal sensory cilia, but not sperm tails. *Curr. Biol.* 13:1687–1696. http://dx.doi.org/10.1016/j.cub.2003.09.025

Schouteden, C., D. Serwas, M. Palfy, and A. Dammermann. 2015. The ciliary transition zone functions in cell adhesion but is dispensable for axoneme assembly in *C. elegans*. *J. Cell Biol.* 210:35–44. http://dx.doi.org/10.1083/jcb.201501013

Shi, J., Y. Zhao, D. Galati, M. Winey, and M.W. Klymkowsky. 2014. Chibby functions in Xenopus ciliary assembly, embryonic development, and the regulation of gene expression. *Dev. Biol.* 395:287–298. http://dx.doi.org/10.1016/j.ydbio.2014.09.008

Sung, C.-H., and M.R. Leroux. 2013. The roles of evolutionarily conserved functional modules in cilia-related trafficking. *Nat. Cell Biol.* 15:1387–1397. http://dx.doi.org/10.1038/ncb2888

Szymanska, K., and C.A. Johnson. 2012. The transition zone: an essential functional compartment of cilia. *Cilia.* 1:10. http://dx.doi.org/10.1186/2046-2530-1-10

Tates, A.1971. Cytodifferentiation during spermatogenesis in Drosophila melanogaster: an electron microscope study. PhD thesis. Rijksuniversiteit Leiden. 1–162.

Vasudevan, K.K., Y.-Y. Jiang, K.F. Lechtreck, Y. Kushida, L.M. Alford, W.S. Sale, T. Hennessey, and J. Gaertig. 2015. Kinesin-13 regulates the quantity and quality of tubulin inside cilia. *Mol. Biol. Cell.* 26:478–494. http://dx.doi.org/10.1091/mbc.E14-09-1354

Vieillard, J., J.-L. Duteyrat, E. Cortier, and B. Durand. 2015. Imaging cilia in Drosophila melanogaster. *Methods Cell Biol.* 127:279–302. http://dx.doi.org/10.1016/bs.mcb.2014.12.009

Villumsen, B.H., J.R. Danielsen, L. Povlsen, K.B. Sylvestersen, A. Merdes, P. Beli, Y.G. Yang, C. Choudhary, M.L. Nielsen, N. Mailand, and S. Bekker-Jensen. 2013. A new cellular stress response that triggers centriolar satellite reorganization and ciliogenesis. *EMBO J.* 32:3029–3040. http://dx.doi.org/10.1038/emboj.2013.223

Voronina, V.A., K. Takemaru, P. Treuting, D. Love, B.R. Grubb, A.M. Hajjar, A. Adams, F.-Q. Li, and R.T. Moon. 2009. Inactivation of Chibby affects function of motile airway cilia. *J. Cell Biol.* 185:225–233. http://dx.doi.org/10.1083/jcb.200809144

Wang, L., T. Piao, M. Cao, T. Qin, L. Huang, H. Deng, T. Mao, and J. Pan. 2013. Flagellar regeneration requires cytoplasmic microtubule depolymerization and kinesin-13. *J. Cell Sci.* 126:1531–1540. http://dx.doi.org/10.1242/jcs.124255

Wei, H.-C., J. Rollins, L. Fabian, M. Hayes, G. Polevoy, C. Bazinet, and J.A. Brill. 2008. Depletion of plasma membrane PtdIns(4,5)P2 reveals essential roles for phosphoinositides in flagellar biogenesis. *J. Cell Sci.* 121:1076–1084. http://dx.doi.org/10.1242/jcs.024927

Williams, C.L., C. Li, K. Kida, P.N. Inglis, S. Mohan, L. Semenec, N.J. Bialas, R.M. Stupay, N. Chen, O.E. Blacque, et al. 2011. MKS and NPHP modules cooperate to establish basal body/transition zone membrane associations and ciliary gate function during ciliogenesis. *J. Cell Biol.* 192:1023–1041. http://dx.doi.org/10.1083/jcb.201012116

Yee, L.E., F.R. Garcia-Gonzalo, R.V. Bowie, C. Li, J.K. Kennedy, K. Ashrafi, O.E. Blacque, M.R. Leroux, and J.F. Reiter. 2015. Conserved genetic interactions between ciliopathy complexes cooperatively support ciliogenesis and ciliary signaling. *PLoS Genet.* 11:e1005627. http://dx.doi.org/10.1371/journal.pgen.1005627